



# HHS Public Access

## Author manuscript

*Adv Funct Mater.* Author manuscript; available in PMC 2018 March 09.

Author Manuscript

Author Manuscript

Author Manuscript

Author Manuscript

Published in final edited form as:

*Adv Funct Mater.* 2013 November 26; 23(44): 5461–5476. doi:10.1002/adfm.201301121.

## Toward Strong and Tough Glass and Ceramic Scaffolds for Bone Repair

**Dr. Qiang Fu,**

Materials Sciences Division, Lawrence Berkeley National Laboratory, Berkeley, CA 94720 (USA)

Corning Inc., Corning, NY 14830 (USA)

**Eduardo Saiz [Prof.]**

Centre for Advanced Structural Materials, Department of Materials, Imperial College London, London, UK

**Mohamed N. Rahaman [Prof.], and**

Department of Materials Science and Engineering, and Center for Bone and Tissue Repair and Regeneration, Missouri University of Science and Technology, Rolla, MO 65409, USA

**Dr. Antoni P. Tomsia**

Materials Sciences Division, Lawrence Berkeley National Laboratory, Berkeley, CA 94720 (USA)

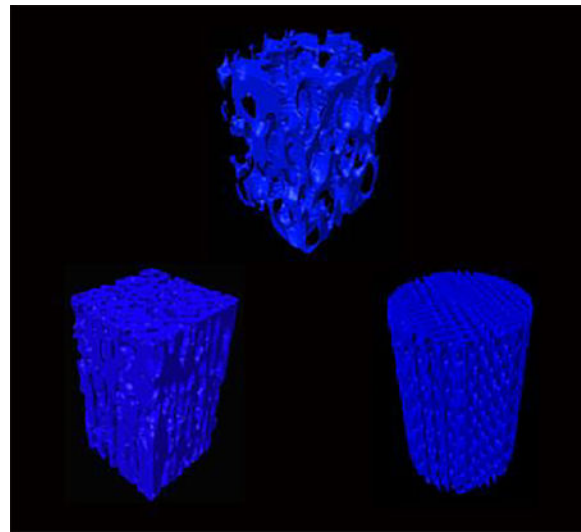
### Abstract

The need for implants to repair large bone defects is driving the development of porous synthetic scaffolds with the requisite mechanical strength and toughness *in vivo*. Recent developments in the use of design principles and novel fabrication technologies are paving the way to create synthetic scaffolds with promising potential for reconstituting bone in load-bearing sites. This article reviews the state of the art in the design and fabrication of bioactive glass and ceramic scaffolds that have improved mechanical properties for structural bone repair. Scaffolds with anisotropic and periodic structures can be prepared with compressive strengths comparable to human cortical bone (100–150 MPa), while scaffolds with an isotropic structure typically have strengths in the range of trabecular bone (2–12 MPa). However, the mechanical response of bioactive glass and ceramic scaffolds in multiple loading modes such as flexure and torsion — as well as their mechanical reliability, fracture toughness, and fatigue resistance — has received little attention. Inspired by the designs of natural materials such as cortical bone and nacre, glass-ceramic and inorganic/polymer composite scaffolds created with extrinsic toughening mechanisms are showing potential for both high strength and mechanical reliability. Future research should include improved designs that provide strong scaffolds with microstructures conducive to bone ingrowth, and evaluation of these scaffolds in large animal models for eventual translation into clinical applications.

### Table of contents

---

Correspondence to: Qiang Fu; Antoni P. Tomsia.



Fundamental understanding of the structure-processing-property relationships of porous glass and ceramic scaffolds is critical for the creation of strong and tough implants. Recent developments in the use of design principles and novel fabrication technologies are paving the way to fabrication of synthetic scaffolds of isotropic, anisotropic and periodic architectures with promising potential for bone repair.

### Keywords

Bioactive glass and ceramics; porous scaffolds; bone tissue engineering; mechanical strength; reliability

## 1. Introduction

Tissue and organ failures resulting from trauma, disease, or aging have been reported to account for half of the annual healthcare expenditures in the US.<sup>[1]</sup> Among them, bone is the second most commonly transplanted tissue with blood being the first.<sup>[2]</sup> Current treatments such as transplantation of tissues and organs; surgical repair; the use of artificial prostheses or mechanical devices; and drug therapy are effective but suffer from limitations.<sup>[1]</sup>

Autografts with optimal osteoconductive, osteoinductive, and osteogenic properties remain the gold standard for bone repair,<sup>[3]</sup> despite the disadvantages of donor site morbidity and limited availability. Bone allografts are alternatives but they suffer from possible transmission of diseases, immune reaction, and uncertain healing to bone. Tissue engineering approaches using an osteoconductive scaffold loaded with growth factors and osteogenic cells have shown great potential for bone repair and regeneration.<sup>[1, 4, 5–7]</sup>

Scaffolds play a critical role by serving as a template for the delivery of growth factors and cell attachment while providing a temporary support for the defect sites.

An implant for bone repair should have a combination of properties that satisfy a stringent set of requirements. Ideally, the implant should be biocompatible,<sup>[8]</sup> bioactive, or biodegradable — with a degradation rate comparable to the rate of new bone formation. The

implant should have a porous three-dimensional (3-D) architecture capable of supporting cell and tissue infiltration, transport of nutrients, and development of capillaries.<sup>[9]</sup> It must have the requisite mechanical properties for supporting loads experienced by the bone to be replaced.<sup>[7, 9–11, 12]</sup> Considerable improvements in scaffold design, fabrication, and evaluation is necessary to meet these stringent requirements, particularly for applications in the repair of load-bearing bone.

## 2. Design of scaffolds: a mechanical perspective

A typical long bone of the limbs is composed of two types of bone, each having a different structural organization: cortical bone, also referred to as compact bone; and trabecular bone, also referred to as cancellous or trabecular bone.<sup>[13]</sup> Composed mostly of an inorganic phase (hydroxyapatite) and an organic phase (collagen), cortical bone has a unique combination of strength and toughness. Cortical bone has a compressive strength of 100–150 MPa in the long direction, and a flexural strength of 135–193 MPa. The fracture toughness,  $K_{1c}$ , of cortical bone (2–12 MPa·m<sup>1/2</sup>) has an upper range that is much higher than the values for most ceramics and inorganic glass (typically  $K_{1c} = 0.5\text{--}5 \text{ MPa}\cdot\text{m}^{1/2}$  for ceramics and 0.5–1 MPa·m<sup>1/2</sup> for glass).

This exceptional combination of mechanical properties is attributed to the hierarchical structure of bone, composed of cascaded arrangements of building blocks at defined length scales (Figure 1).<sup>[13, 14]</sup> Structurally, bone is a composite material, composed of collagen (35 wt% based on dry bone) for flexibility and toughness; carbonated hydroxyapatite (65 wt%) for structural reinforcement, stiffness, and mineral homeostasis; and other non-collagenous proteins for support of cellular functions.<sup>[13, 15]</sup> The architecture of bone, while complex in nature, can be described in terms of up to seven hierarchical levels of organization. These levels include hydroxyapatite crystals (1.5–4.5 nm) and mineralized collagen fibrils at a nanometer scale; a fibril array, its corresponding array patterns and osteons at a micrometer scale; and the cortical/trabecular bone and whole bones at a macroscopic scale.<sup>[14, 16]</sup> The origins of the high fracture-toughness of cortical bone are reported to be a combination of intrinsic and extrinsic toughening mechanisms (Figure 1).<sup>[14]</sup> The intrinsic toughness is due to a plasticity mechanism, operating at a submicrometer scale, involving the molecular uncoiling of collagen molecules, mineralized collagen fibril sliding, and microcracking. The extrinsic toughening mechanisms occur at length scales of ~1–100 μm via crack deflection/twist and crack bridging.<sup>[14, 17]</sup>

Inspired by the impressive properties of natural materials such as cortical bone, researchers are making considerable efforts to mimic the architecture and function of those materials to design new synthetic structures with similar performance. The requirement for high mechanical strength in scaffolds to be used for repairing large segmental bone defect sites is without doubt based on the configurations of the fixation methods: plate fixation, external fixator and intramedullar nail (Figure 2).<sup>[18]</sup> All three fixation methods require scaffolds to carry a portion of the load (plate fixation and external fixator) or almost the entire load (intramedullar nail) from the body weight or daily activities. However, there is no general agreement on the appropriate materials and their mechanical properties required for bone repair due to the complexities involved in clinical implantation, bone/scaffold interaction,

scaffold degradation, tissue ingrowth, and complete healing. From a mechanical perspective, scaffolds for bone tissue engineering applications should have a strength that is similar to, or higher than, that of the bone to be repaired. In addition, the scaffold should have an elastic modulus similar to bone to reduce stress shielding and adequate toughness to prevent its catastrophic failure behavior.<sup>[8, 9, 19, 20]</sup> However, the variability in the architecture and mechanical properties of bone — combined with differences in age, nutritional state, activity (mechanical loading), and disease status of individuals — is a major challenge for the design and fabrication of scaffolds at specific defect sites.

In general, the properties of a scaffold depend mostly on its composition and microstructure. The biodegradable polymers, ceramics, or metal alloys currently used as scaffold materials for tissue engineering in orthopedic applications have a different mechanical response from bone. The use of biodegradable polymer scaffolds for regeneration of load-bearing bones is challenging due to their low mechanical strength.<sup>[21, 22]</sup> Attempts have been made to reinforce the polymers with a biocompatible inorganic phase, commonly hydroxyapatite (HA).<sup>[20, 23, 24]</sup> However, because of a lack of adequate adhesion between the biopolymer and the inorganic phase, the desired mechanical properties of the composite materials are unlikely to be met.<sup>[25]</sup> The lack of a matching degradation rate between the polymer and the inorganic phase also could result in instability of the scaffold and migration of particles *in vivo*.<sup>[26]</sup> Comprehensive reviews on polymer-based scaffolds are available in the literature.<sup>[9, 21]</sup>

Significant efforts have been made to use bioceramics as scaffold materials for large segmental bone defect repair owing to their excellent osteoconductive (bioactive ceramics) and osteoinductive (bioactive glass) properties.<sup>[5, 18, 27, 28]</sup> Despite increasing interest in this group of materials, their process – structure – property relationships have not been well studied. This article focuses on the mechanical properties of this group of inorganic scaffolds that could be potentially used to repair loaded bone defects.

### 3. Scaffold fabrication routes

Although they are brittle, scaffolds fabricated from inorganic materials of calcium phosphate-based bioceramics and bioactive glass have appealing characteristics such as high mechanical strength under compression and excellent biocompatibility for bone tissue engineering. Calcium phosphate-based bioceramics such as hydroxyapatite (HA);  $\text{Ca}_{10}(\text{PO}_4)_6(\text{OH})_2$ ;  $\beta$ -tricalcium phosphate ( $\beta$ -TCP);  $\text{Ca}_3(\text{PO}_4)_2$ ; and biphasic calcium phosphate (BCP) — a mixture of HA and  $\beta$ -TCP — are composed of the same ions as bone, and have received most attention for bone repair applications. Silicon-substituted calcium phosphate has also been used as scaffold materials due to their improved biological performance compared to pure calcium phosphate.<sup>[29]</sup> Properties such as *in vivo* osteoconductivity, bioactivity, and resorbability of this group of materials are dependent upon their Ca/P atomic ratio, crystallographic structure, and porosity (or surface area) and have been reviewed elsewhere.<sup>[30, 31]</sup>

Bioactive glass refers to inorganic glasses with special compositions that react with body fluids *in vivo* to form a surface layer of hydroxyapatite that bonds strongly to hard and soft

tissues.<sup>[32, 33]</sup> Several groups of glasses, based on silicate, borate, and phosphate glass compositions, have been shown to be bioactive.<sup>[32–34]</sup> The mechanism of bioactivity, and the in vitro and in vivo evaluations of bioactive glasses for applications in tissue engineering have been reported in literature.<sup>[26, 32, 33, 35]</sup> The ease of manipulating their structure and chemistry over a wide range, by changing either composition or the processing history (thermal or environmental), makes bioactive glasses very appealing as scaffold materials. Since the discovery of 45S5 bioactive glasses by Hench,<sup>[36]</sup> bioactive glasses have been widely researched and developed for bone repair applications.<sup>[32, 36–38]</sup>

A variety of techniques have been used for the fabrication of bioactive glass and ceramic scaffolds, including sol-gel methods; thermal bonding of particles, fibers, or spheres; polymer foam replication; foaming of suspensions; freeze casting and solid freeform fabrication (SFF). In general, interconnected pores with a pore size (diameter or width) larger than ~100 µm are considered as a minimum requirement for tissue ingrowth and function in porous scaffolds.<sup>[10, 19, 33, 34]</sup> The upper limit of pore size is set by the constraints associated with the mechanical properties of the scaffolds and the dimensions of the pores of the bones to be repaired.<sup>[19]</sup> In addition to porosity and pore size, the shape of the necks between adjacent pores, microporosity in the solid phase and the architecture of the solid phase in the scaffolds are also important for bone ingrowth and mechanical performances.

Despite the diversity of fabrication techniques, scaffolds can generally be grouped into three types based on their microstructure: isotropic, anisotropic, and periodic. Typical microstructures of each group, prepared from 13–93 bioactive glass, are shown in Figure 3. Fabrication techniques used to prepare the scaffolds has been summarized in several published reviews and are not repeated in this article.<sup>[24, 33, 34]</sup>

Isotropic scaffolds are those with a random distribution of pores in three dimensions (Figure 3a). The pore geometry can be either nearly spherical or irregular based on the specific fabrication technique. Typically, the sol-gel,<sup>[39]</sup> polymer foam replication,<sup>[40, 41, 42, 43, 44–46, 47]</sup> and foaming method produce scaffolds composed of spherical pores with interconnected porosity.<sup>[48, 49, 50]</sup> Scaffolds with irregular pores are generally prepared by thermally bonding a mass of particles, short fibers, or microspheres.<sup>[51, 52, 53]</sup> Depending on the specific technique, pore sizes in the range 10–800 µm and a porosity of 24–96% can be achieved in scaffolds. For any given technique, the porosity and pore size can be controlled by the size of the particles, the foaming procedure, or the size of the porogen or template.

A typical feature of anisotropic scaffolds is the presence of an oriented porosity or solid phase in the microstructure (Figure 3b). In addition to the conventional extrusion,<sup>[54]</sup> filament winding,<sup>[55]</sup> electrophoretic deposition,<sup>[56]</sup> wood replication,<sup>[57]</sup> and slip casting methods,<sup>[58]</sup> unidirectional freezing of suspensions is a relatively new technique that has been developed for creating porous materials with an oriented porosity.<sup>[59, 60, 61, 62]</sup> This technique overcomes the limitations such as difficulties in controlling the porosity, pore size, and the solid phase associated with the conventional methods. By controlling the processing parameters such as freezing velocity, solvent composition and particle concentration, HA

scaffolds with unidirectional pores of different morphology and ceramic struts of various features can be obtained<sup>[60, 63]</sup>. Typical pore sizes are in the range of 10–40 µm for scaffolds with a lamellar structure (pore width), and 50–150 µm for scaffold with columnar structure (pore diameter), while the porosity can be in the range of 20–70%.

Periodic scaffolds typically have a microstructure with a regular repeating pattern in at least one plane of the scaffold, and they are commonly fabricated by solid freeform fabrication (SFF) or rapid prototyping technique (Figure 3c).<sup>[12, 64, 65–67]</sup> The pore size, morphology and porosity can be varied over a wide range, but pores of size (width) 100–500 µm and porosity in the range 40–70% have been commonly studied.

#### 4. Mechanical properties

As described in the previous section, scaffolds with a wide range of microstructures can be obtained depending on the materials and fabrication techniques used. In this section, the mechanical properties (compressive strength, flexural strength, fracture toughness, fatigue, and reliability) of those isotropic, anisotropic, and periodic scaffolds are reviewed with special reference to their process-structure-property relationships for improved mechanical performance. The data for ceramics and bioactive glass scaffolds will be considered in separate sections to provide a better understanding of the microstructural effects on properties.

Most previous studies have focused primarily on the evaluation of the strength and elastic modulus of porous bioactive glass and ceramic scaffolds in compression. However, during normal physiological activity, bone in load-bearing sites is subjected to multiple loading modes as well as cyclic loading. Consequently, the response of porous scaffolds in multiple loading modes — such as compression, flexure, and torsion — and the fatigue resistance of the scaffolds are relevant. Bioactive glass and ceramic scaffolds are also brittle, so their resistance to fracture (as determined by their fracture toughness), and evaluation of their mechanical reliability using statistical analysis (Weibull statistics) are relevant to brittle materials. In addition to the mechanical properties of the as-fabricated scaffolds, the degradation of the scaffold material and its effect on the strength of the scaffold in vitro and in vivo are important. The difference in degradation rate of the scaffold materials (for example bioactive glasses of different compositions) has a marked effect on the decrease in mechanical strengths in simulated body fluid (SBF) in vitro.<sup>[44, 68]</sup> In vivo evaluation of true mechanical performances of scaffolds is difficult due to infiltration of tissues into their pores. Therefore, this article focuses on the mechanical properties of the scaffold before implantation in order to better assess the impact of the structure and processing on strength.

It should be noted that not all the mechanical data reported in literature for porous scaffolds have been tested according to methods specified by the American Society for Testing and Materials (ASTM). This is due to the fact that most of the ASTM test methods are based on dense ceramic samples while porosity is required in scaffolds intended for bone tissue engineering. The presence of porosity in scaffolds also makes it difficult to machine them into standard test samples as specified by the ASTM.

## 4.1 Compressive strength

Compression is the most relevant loading mode that a scaffold would be subjected to in vivo, so compression testing is commonly used to evaluate porous scaffolds. Compressive strength is measured on either cubic or cylinder specimens with two parallel and flat loading surfaces according to ASTM.<sup>[69]</sup> Compressive strength is also the most widely reported mechanical property for porous scaffolds due to the ease of sample preparation and testing, and it serves as a preliminary screening test for scaffold selection. A wide range of compressive strengths has been reported for bioactive glass and ceramic scaffolds.

**4.1.1 Compressive strength of bioactive glass scaffolds**—Figure 4 shows data for the compressive strength of bioactive glass scaffolds which were compiled from the literature.<sup>[40, 41, 42, 44, 52, 62, 66, 70]</sup> Several interesting trends can be obtained from these data. First, a wide range of the strength values, 0.2–150 MPa for porosities of 30–95%, is observed (Figure 4a). Most of the data fall within or near the range for trabecular bone. However, a limited number of studies in recent years have reported strengths in the range of cortical bone (100–150 MPa), which indicates that bioactive glass scaffolds could be considered for loaded bone repair.

Second, the strength decreases with an increase in scaffold porosity (Figure 4b). The influence of porosity, as well as the size, geometry, and distribution of the pores, has been shown to influence the mechanical strength of porous ceramics.<sup>[71, 72–74]</sup> An exponential relation between strength and porosity is often observed in porous glass and ceramics:<sup>[71, 72]</sup>

$$\sigma = \sigma_0 \exp(-kP) \quad (1)$$

where  $\sigma$  is the strength porous ceramics;  $\sigma_0$  is the strength of fully dense material;  $k$  is an exponentially determined constant; and  $P$  is the open porosity. A linear correlation for  $\ln \sigma$  versus  $P$  is expressed as following:

$$\ln \sigma = \ln \sigma_0 - kP \quad (2)$$

Despite the difference in pore size and geometry, a simple linear fit to the data for  $\ln \sigma$  versus  $P$  is obtained. From the slope and intercept of the curve both  $\sigma_0$  and  $k$  values can be derived, which are 720 MPa and –7.4, respectively.

The compressive strength,  $\sigma_{cr}$ , of brittle cellular solids (glass and ceramics) with close- and open-cells has been well described by the Gibson and Ashby models:<sup>[75]</sup>

$$\frac{\sigma_{\text{theo}}}{\sigma_{\text{fs}}} = 0.2 \left( \phi \frac{\rho_{\text{foam}}}{\rho_{\text{solid}}} \right)^{3/2} + (1-\phi) \left( \frac{\rho_{\text{foam}}}{\rho_{\text{solid}}} \right) = 0.2 \phi^{3/2} (1-P)^{3/2} + (1-\phi)(1-P) \quad (\text{close-cell}) \quad (3)$$

$$\frac{\sigma_{\text{theo}}}{\sigma_{fs}} = 0.2 \left( \frac{\rho_{\text{foam}}}{\rho_{\text{solid}}} \right)^{3/2} \frac{1 + (t_i/t)^2}{\sqrt{1 - (t_i/t)^2}} = 0.2(1 - P)^{3/2} \frac{1 + (t_i/t)^2}{\sqrt{1 - (t_i/t)^2}} \quad (\text{open-cell}) \quad (4)$$

where  $\sigma_{fs}$  is the modulus of rupture of the struts of the foam;  $\phi$  is the fraction of solid in the cell edge;  $\rho_{\text{foam}}$  and  $\rho_{\text{solid}}$  are the densities of the foam and the fully dense solid, respectively;  $P$  is the porosity of the foam; and  $t_i/t$  is the ratio of the central void size of the struts to the strut size. All three types of scaffolds (isotropic, anisotropic and periodic) have the cellular pore morphology defined by Gibson and Ashby,<sup>[75]</sup> and can be described using their model. An upper and lower theoretical strength of the glass scaffolds can be predicted based on the strength of two most commonly used glass compositions, 13–93 and 45S5.<sup>[34]</sup> As a widely studied scaffold material, 13–93 glass favors the densification of glass struts, resulting in much higher compressive strength than those prepared from 45S5 glass.<sup>[34]</sup> The tensile strength of 13–93 fibers of 93–160 μm (comparable size to glass strut in scaffolds) is reported to be 440 ± 151 MPa,<sup>[76]</sup> while the tensile strength of 45S5 glass fiber (165–310 μm) is 88 ± 32 MPa.<sup>[77]</sup> Therefore, upper theoretical strengths are given by the 13–93 glass with close-cell porosity while lower theoretical strengths are given by the 45S5 glass scaffolds with open-cell porosity (Figure 4b). The strengths of 45S5-derived glass-ceramic scaffold are even lower than the predicted values based on 45S5 glass.<sup>[40, 42]</sup> This is because 45S5 glass crystallizes prior to sintering, which results in a partial densification of its struts. The compressive strengths of the majority of the glass scaffolds fall between these two theoretical limits.

Third, irrespective of glass composition, the scaffold architecture (or microstructure) has a strong effect on strength (Figure 4a). For the same porosity, scaffolds with an oriented or periodic structure (green and pink regions, respectively) show a much higher compressive strength than those with an isotropic structure (purple region). As discussed above, anisotropic and periodic scaffolds are generally fabricated using freeze casting and solid freeform fabrication techniques. These fabrication techniques create scaffolds with an oriented or well-controlled periodic microstructure, which generally leads to high mechanical strength when tested along the pore orientation direction. Additionally, the struts in anisotropic and periodic scaffolds are generally thicker and more uniform than those in isotropic scaffolds. In anisotropic and periodic scaffolds, struts have a uniform diameter of over 100 μm while those in isotropic scaffolds range from tens to several hundred. These thicker struts may also contribute to the higher strengths observed in the anisotropic and periodic scaffolds.

The composition of the glass can also have a strong effect on the mechanical properties of the scaffold. For example, scaffolds of silicate 13–93 bioactive glass with a grid-like microstructure (porosity = 48%) had an average compressive strength of 142 MPa, which was more than twice the average strength (65 MPa) of borate 13–93B3 bioactive glass scaffolds with a similar microstructure.<sup>[68]</sup> The lower strength of the borate glass scaffolds is consistent with previous work in which the compressive strength of silicate 13–93 and borate 13–93B3 scaffolds with a trabecular microstructure was compared.<sup>[44]</sup> For the same

microstructure, the difference in strength between the silicate and borate scaffolds is related to the strength of the Si–O and B–O bonds in the individual glasses.

**4.1.2 Compressive strength of bioactive ceramic scaffolds**—In general, the compressive strength data for the bioactive ceramic scaffolds (such as HA,  $\beta$ -TCP, BCP and Actifuse) show trends that are similar to those described in the previous section for the bioactive glass scaffolds.<sup>[46, 47, 48, 49, 61, 63, 65, 78, 79–81]</sup> The major features of the data on bioactive ceramics will only be discussed briefly. First, the compressive strengths of the bioactive ceramic scaffolds are in the range 0.01–145 MPa for porosity values of 31–96% (Figure 5a), which indicate that these scaffolds could be applied in loaded or non-loaded bone repair. Second, strength decreases approximately exponentially with increasing porosity (Figure 5b). A plot of  $\ln \sigma$  versus  $P$ , based on Equation (2), gives  $k = 9$  and  $\sigma_0 = 1075$  MPa; the value of  $\sigma_0$  is in the range of compressive strengths reported for sintered HA (500–1000 MPa), and is much higher than that of  $\beta$ -TCP (460–687 MPa).<sup>[32]</sup> The upper and lower theoretical strengths are predicted based on Equations (3) and (4), respectively. Tensile strength of HA in the range of 79–196 MPa is used for the strength prediction.<sup>[30]</sup> The majority of the compressive strength values for bioactive ceramic scaffolds fall between these two theoretical limits (Figure 5b).

Third, the microstructure of a scaffold has a strong impact on its compressive strength. Scaffolds with oriented or periodic microstructures show much higher compressive strengths than those with isotropic microstructures (Figure 5a). For HA scaffolds with the same porosity (56%), oriented scaffolds prepared by unidirectional freezing of suspensions had a compressive strength of 65 MPa, compared to a value of 0.85 MPa for scaffolds with a “trabecular” microstructure prepared by a polymer foam replication technique.<sup>[47, 63]</sup> Fourth, the material composition of the scaffold also has a strong influence on scaffold strength. For periodic scaffolds with the same porosity of 40% prepared using a direct ink writing technique, the compressive strength of HA scaffolds (50 MPa) was almost three times as high as that of  $\beta$ -TCP scaffolds (14 MPa).<sup>[65]</sup> The higher intrinsic fracture strength of the HA filament (68 MPa) compared to that of the  $\beta$ -TCP filament (27 MPa) in the scaffolds accounts for their difference in compressive strength.

To summarize at this stage, the compressive strength of both bioactive glass and ceramic scaffolds falls within the range of that for cortical and trabecular bone, indicating their potential for applications in non-loading and load-bearing sites. The compressive strength is strongly dependent on the porosity, microstructure, and material composition of the scaffold. Scaffolds with an oriented microstructure or a periodic microstructure show much higher compressive strength than scaffolds with an isotropic microstructure; and they can be considered for repair of loaded as well as non-loaded bone.

## 4.2 Flexural strength

The flexural strength of ceramic materials is determined by three-point or four-point bending of beam-shaped specimens according to testing procedures approved by the ASTM.<sup>[82]</sup> Because beam-shaped specimens are more difficult to prepare than the cylindrical or cube-shaped specimens used in compression tests, particularly for porous materials, only limited

data are available in the literature for the flexural strength of bioactive glass and ceramic scaffolds. Flexural strength data for bioactive glass scaffolds with isotropic and periodic microstructures are shown Figure 6a, while data for isotropic HA scaffolds are shown in Figure 6b. Flexural strengths span almost two orders of magnitude, in the range 0.4–41 MPa for bioactive glass scaffolds,<sup>[83, 84]</sup> and 0.4–24 MPa for ceramic scaffolds.<sup>[53, 79, 85]</sup> The flexural strength decreases with increasing porosity, but dependence on porosity is not very strong in the porosity range shown (~40–90%). Although some of the reported values are in the range for human trabecular bone (10–20 MPa), all the values are well below those for cortical bone (135–193 MPa).<sup>[34]</sup> Failure typically occurs in the regions of the scaffold that experience tensile stress during the bending test. Brittle materials such as glass and ceramics are weak in tension, so they typically have flexural strengths that are much lower than their typical compressive strength.<sup>[20, 65]</sup> However, as similarly observed to be the case with compressive strength (Figures 4 and 5), bioactive glass scaffolds with a periodic microstructure prepared by a direct ink writing technique show a much higher flexural strength than the scaffolds with an isotropic scaffold (Figure 6a).

#### 4.3 Tensile strength

The tensile strength of a ceramic material is tested on dumbbell-shaped specimens placed in the grips of a tensile testing machine according to ASTM.<sup>[82]</sup> Fabrication of tensile test specimens is complex, usually requiring numerically controlled machining and a large amount of sample material removal from a cylinder, making it difficult to prepare samples from porous scaffolds. As an alternative to the uniaxial tensile test, an indirect measurement of tensile strength of brittle materials is conducted by diametral compression of discs and annuli.<sup>[86]</sup> A limited number of studies have been conducted to investigate the tensile strength of porous calcium phosphate ceramic scaffolds.<sup>[48, 87, 88]</sup> The majority of the tensile strengths of the isotropic ceramic scaffolds (0.4–10 MPa for porosity of 35–85%) fall within the range of trabecular bone (1–5 MPa), as depicted in Figure 7. The values are well below those for cortical bone (50–151 MPa).<sup>[34]</sup> Given that the isotropic scaffolds are generally weaker than anisotropic and periodic scaffolds, the latter two types of scaffolds will likely exhibit higher tensile strength. Testing of the diametral tensile strength of periodic glass scaffolds is under way in our lab. Further studies are needed to find new strategies to improve the tensile strength of both glass and ceramic scaffolds.

#### 4.4 Mechanical reliability (Weibull modulus)

The strength of brittle materials (glass and ceramics) typically has a considerable scatter due to variation in the size, position, and orientation of the flaws responsible for failure. A quantitative evaluation of uniaxial strength (compressive, flexural and tensile) data and the estimation of the failure probability (or the reliability) are commonly performed using a Weibull statistical analysis, as specified by ASTM.<sup>[89]</sup> The Weibull distribution is given as a cumulative distribution:<sup>[89, 90]</sup>

$$P_f = 1 - \exp\left[-\left(\frac{\sigma}{\sigma_\theta}\right)^m\right] \quad (5)$$

where  $P_f$  is the probability of failure at a stress  $\sigma$ ,  $\sigma_0$  is Weibull characteristic strength, and  $m$  is the Weibull modulus (or the shape parameter). The Weibull modulus,  $m$ , can be obtained from the plot of  $\ln[-\ln(1-p)]$  versus  $\ln\sigma$ , the slope of which gives the  $m$  value. A higher Weibull modulus indicates a narrower distribution in strength and therefore a more reliable material. The characteristics strength,  $\sigma_0$ , is the strength that corresponds to a  $P_f$  of 63.2%, or a value of zero for  $\ln[-\ln(1-p)]$ . To get an unbiased estimate of the failure probability, the recommended number of specimens is between 20–30.<sup>[89, 91]</sup>

A comprehensive investigation of bulk HA fractured in biaxial flexure has been performed to understand the effect of porosity on its strength and mechanical reliability.<sup>[92]</sup> Porosity has a strong impact on the Weibull modulus ( $m$ ), fracture strength and elastic modulus in sintered HA. A few studies have used the Weibull distribution to evaluate the reliability of porous glass and ceramic scaffolds.<sup>[65, 80, 84]</sup> For periodic ceramic (HA and  $\beta$ -TCP) scaffolds prepared using a direct ink writing technique, a Weibull modulus in the range of 3.2–9.3 has been reported in compression.<sup>[65, 80]</sup> Bioactive glass (13–93) scaffolds with a periodic microstructure prepared by a similar method have a Weibull modulus of 6.0 and 5.3 in compression and three-point bending tests, respectively. Isotropic glass-ceramic scaffolds prepared from a CaO–Al<sub>2</sub>O<sub>3</sub>–P<sub>2</sub>O<sub>5</sub> glass were reported to have a Weibull modulus in the range 3–8 in four-point bending tests.<sup>[84]</sup>

The fracture mode of bioactive ceramic scaffolds has been analyzed using different modeling tools to improve both the scaffold strength and reliability.<sup>[80, 93, 94, 95]</sup> A two-scale model has been used to investigate the mechanical behavior of periodic HA and TCP scaffold.<sup>[93]</sup> The Sanchez-Palencia's theory of periodic homogenization was used to link the ceramic strut- and scaffold-scales while the failure strength data of the ceramic strut was analyzed using a Weibull distribution.<sup>[90, 96]</sup> A finite element modeling (FEM) on the stress field of periodic bioactive HA and  $\beta$ -TCP scaffolds indicates a maximum tensile stress located close to the joints of ceramic struts. These stress concentration sites are responsible for crack initiation and propagation in the scaffold under a compressive load and strut failure due to brittle crushing.<sup>[95]</sup> In addition to the maximum tensile stress, the presence of the largest surface flaws on the strut surface also contributes to crack initiation.<sup>[95]</sup> By infiltrating the scaffold with a biodegradable polymer, both the strength and mechanical reliability (Weibull modulus) are significant improved due to the sealing of pre-existing surface flaws on the ceramic strut and the partial transfer of stress to the polymer.<sup>[80]</sup>

#### 4.5 Toughness

Sudden and catastrophic failure at high stress levels in ceramic materials limits their structural applications and remains an engineering challenge.<sup>[20, 38, 74]</sup> Porous scaffolds intended for implantation in load-bearing bone defects are usually subjected to loading from the body weight and daily activities; therefore, in addition to strength and elastic modulus, other mechanical properties such as fracture toughness and reliability are of crucial importance.

A strong and tough scaffold with appropriate porosity is the ideal candidate for applications in load-bearing sites. However, in most engineering materials, strength and toughness are mutually exclusive properties.<sup>[97]</sup> As discussed above, both bioactive glass and ceramic

scaffolds with anisotropic and periodic structures have sufficient compressive strength to make them appealing for applications in load-bearing sites (Figures 4 and 5). However, their intrinsic brittleness or low resistance to crack propagation limits their use in these applications.

Commonly, the resistance of a material to crack propagation is measured in terms of an engineering parameter called the fracture toughness, denoted  $K_{IC}$ .<sup>[74, 98]</sup> As depicted in Ashby's plot for yield strength versus fracture toughness (Figure 8), engineering oxide glass and ceramics are located at the bottom right corner with high strength and low toughness, while bulk metallic glass (BMG) is at the top right corner with high strength and high toughness.<sup>[97, 99]</sup> From a mechanical performance perspective, BMG is an attractive scaffold material.<sup>[100, 101]</sup> However, high fabrication cost and the presence of elements known to cause adverse biological reactions currently prevent the extensive use of amorphous metals in hard-tissue prosthesis.<sup>[101]</sup> On the other hand, an inherently low fracture toughness (typically  $K_{IC} = 0.5\text{--}5 \text{ MPa}\cdot\text{m}^{1/2}$  for ceramics and  $0.5\text{--}1 \text{ MPa}\cdot\text{m}^{1/2}$  for oxide glass and ceramics) makes them very sensitive to the presence of small defects and flaws ( $\sim 10 \mu\text{m}$ ). They typically fail catastrophically when subjected to tensile or flexural stresses far lower than their compressive strength.<sup>[102, 103]</sup> A comprehensive quantification of the "brittle behavior" or toughness of porous glass and ceramic scaffolds is a prerequisite to their application in load-bearing sites. Fracture toughness, work of fracture, and Weibull modulus are the widely accepted parameters for quantifying the brittleness of ceramics.

Standard test methods for measuring the fracture toughness of brittle materials are specified by the ASTM.<sup>[104]</sup> Typically, specimens in the shape of a beam containing a sharp notch or a crack are loaded in three-point or four-point flexure. The low strength of some bioactive glass scaffolds often exacerbates difficulties in machining porous specimens into standard test bars with specific size and geometry.

Fracture toughness of brittle porous materials is analyzed using a continuum linear elastic solution for the stress field in front of a crack tip. The analyses assume that the crack depth is much larger than the cell size.<sup>[105]</sup> The pore size in glass and ceramic scaffolds is generally in the range of  $100\text{--}500 \mu\text{m}$ . A pre-crack length of over 1 mm (a few times of the cell size) is required to satisfy the conditions for applicability of linear fracture mechanics.<sup>[106]</sup> A propagating crack is modeled as passing from cell to cell by transversely fracturing the strut. The crack-tip blunting effect occurs as it passes through the solid strut into an open pore.<sup>[105, 107]</sup> The fracture toughness of brittle porous ceramics (isotropic structure) made of  $\text{Al}_2\text{O}_3$ ;  $\text{Al}_2\text{O}_3\text{-ZrO}_2$ ; alumina-mullite<sup>[108]</sup>;  $\text{SiC}$ <sup>[107]</sup>; and cordierite has been tested.<sup>[106, 109]</sup> Only a few studies on the fracture toughness testing of porous glass and ceramic scaffold are available in the literature because of the difficulties in preparing large test specimens from weak scaffolds.<sup>[84]</sup> Fracture toughness values in the range of  $0.2\text{--}0.6 \text{ MPa}\cdot\text{m}^{1/2}$  are obtained for an isotropic glass ( $\text{CaO-Al}_2\text{O}_3-\text{P}_2\text{O}_5$ ) scaffold (porosity: 58–70% and pore size: 100–300  $\mu\text{m}$ ).<sup>[84]</sup> Although these values are much lower than that for cortical bone (2–12  $\text{MPa}\cdot\text{m}^{1/2}$ ), they are in the upper range for trabecular bone (0.1–0.8  $\text{MPa}\cdot\text{m}^{1/2}$ ).

A simple measure of the fracture toughness of porous scaffolds may be the work of fracture,  $\gamma_{wof}$ ; i.e., the total energy consumed to produce a unit area of fracture surface during

complete fracture.<sup>[110]</sup> Several studies have used the work of fracture to evaluate the toughness of porous glass and ceramic scaffolds.<sup>[83, 111, 112]</sup> However, the work of fracture can only be used for comparisons within a given study: This is because it is not a true material property and it may vary due to the differences in sample dimension, sample geometry, and testing conditions.

#### 4.6 Fatigue resistance

One of the primary causes of bone fracture in humans is repetitive and cyclic loading of bone during daily living.<sup>[113]</sup> Stress fracture, which is caused by prolonged and intense loading; and fragility fracture, caused by a reduction of bone strength due to osteoporosis, are both reported to occur in the trabecular bone region.<sup>[114]</sup> Therefore, in addition to the investigation of sudden, catastrophic failure, investigation of fatigue resistance in scaffolds for load-bearing applications is essential for a safe design. Fatigue in glass and ceramics is a term used to measure processes that lead to degradation of mechanical properties over time.<sup>[115]</sup> Two types of fatigue have been observed in glass and ceramic materials: (1) slow crack growth resulting from stress-corrosion cracking; (2) cyclic fatigue resulting from fatigue-crack propagation.<sup>[116]</sup>

**4.6.1 Slow crack growth**—Slow crack growth in glass and ceramics refers to propagation of subcritical-sized cracks at low rates that can cause delayed failure of ceramic materials when the flaw size reaches a critical value. Standard tests for measuring slow crack growth under constant stress (static fatigue) and constant stress rates (dynamic fatigue) for ceramic materials are specified by the ASTM.<sup>[117]</sup> The analysis of subcritical crack growth — crack propagation for stress intensity factor ( $K_I$ ) lower than  $K_{IC}$  — is of engineering importance for the safe design of structural ceramics, particularly those in corrosive environments.<sup>[74]</sup> Stress-assisted reaction (stress corrosion crack growth) is the principal mechanism for subcritical crack propagation in ceramics.<sup>[74]</sup> Both bioactive glass and ceramics are sensitive to slow crack growth.<sup>[118, 119, 120–122]</sup> Slow crack growth in HA at very low  $K_I$  is believed to result from water absorption on the surface crack and a corresponding decrease in surface energy.<sup>[118]</sup> Studies have confirmed that there is considerably less fatigue resistance for HA in liquid solutions than in air.<sup>[120, 121]</sup> For bioactive glasses, stress corrosion is caused and controlled by a chemical reaction between water and the glasses, i.e., the water attack on the Si-O network.<sup>[122, 123]</sup> The presence of open porosity in a porous HA reduces fatigue resistance considerably in comparison to that in dense ceramics.<sup>[120]</sup> There is as yet no systematic understanding of the impact of microstructure and porosity on slow crack growth in bioactive glass and ceramic scaffolds. Given that these scaffolds may be applied in load-bearing sites in body fluid, a comprehensive evaluation of their fatigue resistance under static and dynamic testing conditions is necessary.

**4.6.2 Cyclic fatigue**—Repetitive, cyclic fatigue related bone failure has been reported clinically after prolonged or rigorous exercise.<sup>[113]</sup> Fatigue performance under cyclic compression and bending testing of trabecular and cortical bones has been extensively investigated,<sup>[124, 125]</sup> and the gradual loss of stiffness and strength throughout cyclic loading resulting from fatigue damage accumulation is hypothesized as the fatigue failure mechanism in bone.<sup>[124]</sup> Evidence shows that both glass and ceramic materials undergo

mechanical degradation under cyclic fatigue loading.<sup>[74, 116]</sup> The cyclic fatigue crack growth rate,  $da/dN$ , can be quantified using a simple Paris power-law relationship of the form:<sup>[126]</sup>

$$\frac{da}{dN} = C(\Delta K)^m \quad (6)$$

where  $a$  is the crack length;  $N$  is the number of cycles of stress;  $K$  is the stress intensity range ( $K = K_{max} - K_{min}$ ); and  $C$  and  $m$  are the fatigue growth exponent and coefficient, respectively.

To date, a limited number of investigations have been carried out on the cyclic fatigue behavior of either dense or porous bioactive glasses and ceramic materials.<sup>[87, 127]</sup> A comparison study of fatigue crack growth in human enamel and HA subjected to mode I cyclic load indicated that a significantly lower driving force (~0.13 MPa·m<sup>1/2</sup>) is required for crack initiation in HA than in enamel (~0.35 MPa·m<sup>1/2</sup>), and that both HA and enamel exhibit similar sensitivity to crack growth ( $m = 7.9$  and  $7.7$  for HA and enamel, respectively). However, the average fatigue crack growth coefficient ( $C$ ) of HA is significantly larger than enamel ( $C = 2.0$  and  $0.00087$  [mm/cycle] × [MPa·m<sup>1/2</sup>]<sup>-m</sup> for HA and enamel, respectively). The lack of toughening mechanisms such as microcracking, crack bridging, crack deflection, and crack bifurcation in HA when compared to enamel results in much less cyclic fatigue resistance in sintered ceramic material.<sup>[127]</sup> Another study on the cyclic fatigue resistance of isotropic HA scaffolds was conducted using a diametral compression test in Hank's solution.<sup>[87]</sup> A decrease of 60% in strength was observed in scaffolds fatigued in that solution for  $9 \times 10^5$  cycles. Fatigue crack growth plus stress corrosion in the liquid solution are believed to account for the decrease in strength.<sup>[87]</sup> The cyclic nature of in vivo loading makes it essential to evaluate the cyclic-fatigue resistance of porous scaffolds. The limited fatigue resistance of both dense and porous HA highlights the significance of the development of strong scaffolds for application in load-bearing sites.

Based on the discussions of strength, toughness, reliability and fatigue resistance, it is clear that compressive strength is not a controlling factor limiting application of some types of (anisotropic and periodic) scaffolds in load-bearing sites. Although there is no consensus on the required set of mechanical characterization tests on scaffolds for bone regeneration, the compiled strength data indicate that compressive strength should remain a primary screening test for scaffold selection but it should be supplemented with flexural and tensile strength testing. The examination of the strength data using Weibull statistical analysis is important for the evaluation of mechanical reliability. Additionally, toughness and fatigue resistance tests can provide valuable information for scaffolds intended for use in large loaded bone sites.

To date, applications for these scaffolds are still constrained by the intrinsic low-fracture toughness of their constituent materials. Further improvements on the toughness of scaffolds utilizing extrinsic toughening mechanisms are being explored. The properties of strong and tough natural biological materials such as bone and nacre are inspiring new approaches in the design of strong yet tough scaffolds for bone tissue engineering.

#### 4.7 Bio-inspired toughening mechanisms

Biological mineralized composites such as bone, dentin, and nacre have a high resistance to crack propagation when subjected to applied loads because they have a combination of high strength and toughness.<sup>[128]</sup> As discussed above, extrinsic toughening mechanisms, such as microcracking, crack bridging, and deflection, are the primary factors contributing to the high fracture toughness of human cortical bone (Figure 1).<sup>[14]</sup> Inspired by the toughening mechanisms in biological materials, various approaches have been taken to toughen scaffold materials and to develop organic/inorganic composites. The first approach comes from creation of a tougher scaffold material, toughened by microstructure control and/or the addition of reinforcing phase(s).<sup>[103, 129]</sup> Glass-ceramic A-W is a good example demonstrating the importance of the microstructure and reinforcing phase on its strength and toughness.<sup>[130]</sup> Through careful control of the heat treatment, the parent glass ( $\text{MgO}\text{-CaO}\text{-SiO}_2\text{-P}_2\text{O}_5\text{-CaF}_2$  system) can be crystallized into an apatite-glass or apatite-wollastonite-glass system. With the increasing crystalline phase content from 0 to 72 wt%, the fracture toughness of the material increased from 0.8 to 1.2 and  $2.0 \text{ MPa}\cdot\text{m}^{1/2}$ , which in turn resulted in an increase of its bending strength from 70 to 90 and 200 MPa. Crack deflection by the formation of wollastonite crystals on the glass-ceramic surface is reported to account for the significant increase in fracture toughness.<sup>[131]</sup> Experiments designed to understand of the toughening mechanisms in glass-ceramics were conducted by initiating cracks in a controlled manner using the Vickers indentation method.<sup>[132]</sup> Three types of glass-ceramics containing leucite, lithium disilicate, and apatite were investigated. Crack bridging and crack deflection were determined to be the most potent toughening mechanisms (Figure 9),<sup>[132]</sup> and both were also found to be the key extrinsic toughening mechanisms of bone (Figure 1).<sup>[14, 17]</sup> The formation of an interlocking microstructure and the high crystalline content of lithium disilicate glass-ceramics produced a crack deflection toughening mechanism and also the highest fracture toughness ( $2.7 \text{ MPa}\cdot\text{m}^{1/2}$ ).<sup>[132]</sup> The combination of high strength and toughness in glass-ceramics has generated wide interest for development of new glass-ceramic materials.<sup>[32, 133]</sup> Although the fracture toughness values ( $2\text{-}3 \text{ MPa}\cdot\text{m}^{1/2}$ ) of most bioactive glass-ceramics are in the lower range for cortical bone ( $2\text{-}12 \text{ MPa}\cdot\text{m}^{1/2}$ ), they are definitely much tougher than either bioactive glass or ceramics ( $K_{IC}$  in the range of  $0.5\text{-}1 \text{ MPa}\cdot\text{m}^{1/2}$ ).<sup>[103]</sup> It should be noted that not all the glass-ceramic scaffolds can have a combination of high strength and toughness.<sup>[132]</sup> For example, the fracture toughness of sintered 45S5 glass-ceramics is not high ( $0.9\text{-}1.1 \text{ MPa}\cdot\text{m}^{1/2}$  within the range of values for glass  $0.5\text{-}1.0 \text{ MPa}\cdot\text{m}^{1/2}$ ),<sup>[134]</sup> and the isotropic glass-ceramic scaffold derived from 45S5 glass has a very low mechanical strength.<sup>[40, 42]</sup> High toughness is only obtained in glass-ceramics with interlocking structure and high crystalline content, which provides effective and efficient extrinsic toughening mechanisms.<sup>[132]</sup> Considering the high strength achieved in both anisotropic and periodic scaffolds (as discussed in Section 4.1 and 4.3), scaffolds made of glass-ceramics with extrinsic toughening mechanisms may be potent candidates for load-bearing site applications.

The second approach attempts to mimic bone structure, which is mainly composed of organic fibrils and inorganic HA, by coating a porous scaffold with a biodegradable polymer that serves as an organic phase to toughen the inorganic portion. As measured by work of fracture, significant increases in toughness have been reported for isotropic scaffolds made

Author Manuscript  
Author Manuscript  
Author Manuscript  
Author Manuscript

of bioactive glass and ceramics. By coating isotropic ceramic (alumina and biphasic calcium phosphate) scaffolds with polycaprolactone (PCL), a 7- to 13-fold increase in work of fracture has been reported.<sup>[111]</sup> Similar findings were also observed in isotropic glass scaffolds toughened by biodegradable polymers poly(D,L-lactic acid); PDLLA;<sup>[83, 135]</sup> poly(3-hydroxybutyrate); P(3HB);<sup>[112]</sup> alginate;<sup>[136]</sup> and PCL.<sup>[34]</sup> Upon compression, polymer-toughened scaffolds exhibit a “plastic” deformation with a gradual failure mode, rather than “brittle” behavior with catastrophic failure.<sup>[34]</sup> The primary energy dissipation mechanism is believed to be PCL fibril extension and crack bridging on the strut surface. However, enhanced toughening by the use of a polymer coating is observed primarily in isotropic scaffolds, which are generally much weaker than anisotropic and periodic scaffolds. Despite the increase in the work of fracture, their strength is much lower than that of cortical bone and their brittleness is still maintained after the degradation of the polymer coating.<sup>[83, 111, 112, 135, 136]</sup> Furthermore, from a biological perspective, the presence of the polymer coating on the bioactive glass and ceramics reduces the bioactivity of the scaffold.<sup>[26]</sup>

A third approach focuses on the creation of engineered polymer/ceramic composites with a “brick and mortar” structure similar to that of nacre (Figure 10a). In nacre, the “bricks” are platelets of the mineral aragonite comprising around 95 vol% of the structure and contributing to its high strength, while the “mortar” is an organic biopolymer that provides extrinsic and intrinsic toughening mechanisms.<sup>[137]</sup> By infiltrating an anisotropic Al<sub>2</sub>O<sub>3</sub> scaffold (fabricated using the freeze casting technique) with an organic phase (poly(methyl methacrylate), PMMA) shown in Figure 10b, the resultant composite scaffold exhibits a similar mechanical behavior to that of nacre (Figure 10c and d), resulting in a flexural strength of ~200 MPa and fracture toughness of 30 MPa·m<sup>1/2</sup>, comparable to that of aluminum alloys.<sup>[138]</sup> This anisotropic composite scaffold meets the mechanical requirements for applications in load-bearing bone sites. The high toughness is due to the presence of several extrinsic toughening mechanisms including microcracking, crack bridging, and crack deflection. The drawback of the method is the formation of a bulk scaffold, which does not have sufficient porosity for the ingrowth of new tissue/bone. However, by choosing a biodegradable polymer with a suitable degradation rate, pores may be formed as the polymer degrades, while at the same time new tissue/bone can infiltrate the scaffold, replacing the original polymer to function as a new “lubricant” phase.

The fourth approach involves the development of inorganic/organic hybrid scaffolds using a modified sol-gel process in which a degradable polymer is introduced in the sol stage to form interlocking polymer chains.<sup>[26, 139]</sup> The process enables the formation of inorganic (silica) network around polymer molecules, leading to molecular-level interactions. Due to the presence of this fine-scale interaction, the bioactive hybrid would have both bioactivity and toughness.<sup>[140]</sup> A monolith of sol-gel hybrid, “star-gel” composed of an organic core surrounded by alkoxy silane groups is reported to have a toughness of 2.8 MPa·m<sup>1/2</sup>.<sup>[141]</sup> However, the strength of the hybrid scaffold is generally within the range of trabecular bone and is not suitable for applications in loading sites.<sup>[26]</sup>

As measured by the toughness, the available scaffolds are much more “brittle” than cortical bone. Although recent work has demonstrated success in development of anisotropic and

periodic scaffolds with high mechanical strength, challenges remain in the development of new materials and methods to toughen the bioactive glass and ceramic scaffolds for applications in load-bearing sites.

## 5. Biological performance

The ability of bioactive glass and ceramic scaffolds to support cell proliferation and function in vitro and tissue ingrowth in vivo has been shown in numerous studies.<sup>[33, 34, 142]</sup> In vivo evaluations of bioactive glass and ceramic scaffolds have been conducted in animal models including dogs,<sup>[28]</sup> rabbits,<sup>[67, 143]</sup> rats,<sup>[33, 45]</sup> and in clinical practice.<sup>[5–7, 28]</sup> In a clinical study, isotropic HA scaffolds seeded with bone marrow stromal were implanted into long bone defects (4 cm in length) in patients (Figure 11).<sup>[5, 7]</sup> A complete fusion between the implant and the host bone was found 5–7 months after surgery and good integration was maintained through all follow-ups (7 years post-surgery). The study concluded that high porosity and a high degree of interconnection in HA scaffolds are required for vascularization and new bone formation. However, the low mechanical strength of HA scaffolds is reported to be one of the most important obstacles in the practice,<sup>[7]</sup> underscoring the urgent need to develop scaffolds with better mechanical properties before they will be suitable for widespread clinical applications.

## 6. Conclusions and future directions

The fabrication, mechanical properties, and biological performance of bioactive glass and ceramic scaffolds were reviewed here with an emphasis on the mechanical behavior of scaffolds for applications in the repair of loaded bone defects. Scaffolds with isotropic, anisotropic, and periodic structures have been produced with a variety of fabrication techniques and reported in the literature. Their mechanical performance indicates that strength is not a limiting factor in the use of bioactive glass and ceramic scaffolds for load-bearing bone repair, an observation seldom recognized by researchers and clinicians. Scaffolds with anisotropic and periodic structures exhibit compressive strength comparable to that of cortical bone (100–150 MPa), while the strength of those with isotropic structure is in the range of trabecular bone (2–12 MPa). However, use of inorganic scaffolds is still limited by their inherent brittleness (low fracture toughness in the range of 0.5–1 MPa·m<sup>1/2</sup>). With designs inspired by those of natural biological materials such as cortical bone and nacre, glass-ceramic and inorganic/polymer composite scaffolds toughened by extrinsic mechanisms have demonstrated great potential in achieving both high strength and toughness. Future research should focus on development of strong yet tough scaffolds using techniques that optimize structure, and on the evaluation of these scaffolds in large animal models and in clinical practice.

## Acknowledgments

This work was supported by the National Institutes of Health/National Institute of Dental and Craniofacial Research (NIH/NIDCR) Grant No. 1R01DE015633. We acknowledge the support of the dedicated X-ray tomography beamline 8.3.2 at the Advanced Light Source, funded by Department of Energy under contract No. DE-AC02-05CH11231.

## References

1. Persidis A. *Nat Biotechnol*. 1999; 17:508. [PubMed: 10331816]
2. Boyce T, Edwards J, Scarborough N. *Orthop Clin N Am*. 1999; 30:571. Van Heest A, Swiontkowski M. *Lancet*. 1999; 353:SI28.
3. Cypher T, Grossman J. *J Foot Ankle Surg*. 1996; 35:413. [PubMed: 8915864]
4. Langer R, Vacanti JP. *Science*. 1993; 260:920. [PubMed: 8493529] Reichert JC, Cipitria A, Epari DR, Saifzadeh S, Krishnakant P, Berner A, Woodruff MA, Schell H, Mehta M, Schuetz MA, Duda GN, Hutmacher DW. *Sci Transl Med*. 2012; 4
5. Quarto R, Mastrogiamomo M, Cancedda R, Kutepov SM, Mukhachev V, Lavroukov A, Kon E, Marcacci M. *New Engl J Med*. 2001; 344:385. [PubMed: 11195802]
6. Vacanti CA, Bonassar LJ, Vacanti MP, Shufflebarger J. *New Engl J Med*. 2001; 344:1511. [PubMed: 11357154]
7. Marcacci M, Kon E, Moukhachev V, Lavroukov A, Kutepov S, Quarto R, Mastrogiamomo M, Cancedda R. *Tissue Eng*. 2007; 13:947. [PubMed: 17484701]
8. Giannoudis PV, Dinopoulos H, Tsiridis E. *Injury-International Journal of the Care of the Injured*. 2005; 36:20.
9. Hutmacher DW. *Biomaterials*. 2000; 21:2529. [PubMed: 11071603]
10. Hollister SJ, Maddox RD, Taboas JM. *Biomaterials*. 2002; 23:4095. [PubMed: 12182311]
11. Liu X, Ma PX. *Ann Biomed Eng*. 2004; 32:477. [PubMed: 15095822] Salgado AJ, Coutinho OP, Reis RL. *Macromolecular Bioscience*. 2004; 4:743. [PubMed: 15468269] Sittiger M, Hutmacher DW, Risbud MV. *Current Opinion in Biotechnology*. 2004; 15:411. [PubMed: 15464370] Chen VJ, Smith LA, Ma PX. *Biomaterials*. 2006; 27:3973. [PubMed: 16564086]
12. Hollister SJ. *Nat Mater*. 2005; 4:518. [PubMed: 16003400]
13. Fratzl P, Gupta HS, Paschalis EP, Roschger P. *J Mater Chem*. 2004; 14:2115.
14. Launey ME, Buehler MJ, Ritchie RO. *Annu Rev Mater Res*. 2010; 40:25.
15. Athanasiou KA, Zhu CF, Lanctot DR, Agrawal CM, Wang X. *Tissue Eng*. 2000; 6:361. [PubMed: 10992433]
16. Weiner S, Wagner HD. *Annu Rev Mater Sci*. 1998; 28:271.
17. Nalla RK, Kinney JH, Ritchie RO. *Nat Mater*. 2003; 2:164. [PubMed: 12612673]
18. Reichert JC, Saifzadeh S, Wullschleger ME, Epari DR, Schütz MA, Duda GN, Schell H, van Griensven M, Redl H, Hutmacher DW. *Biomaterials*. 2009; 30:2149. [PubMed: 19211141]
19. Karageorgiou V, Kaplan D. *Biomaterials*. 2005; 26:5474. [PubMed: 15860204]
20. Wagoner Johnson AJ, Herschler BA. *Acta Biomater*. 2011; 7:16. [PubMed: 20655397]
21. Hayashi T. *Progress in Polymer Science*. 1994; 19:663. Agrawal CM, Ray RB. *J Biomed Mater Res*. 2001; 55:141. [PubMed: 11255165] Griffith LG. *Acta Mater*. 2000; 48:263.
22. Lee KY, Mooney DJ. *Chemical Reviews*. 2001; 101:1869. [PubMed: 11710233] Varghese S, Elisseeff JH. *Polymers for Regenerative Medicine*. 2006; 95Reis, RL. *Natural-based polymers for biomedical applications*. Woodhead Publishing Limited; Cambridge, UK: 2008.
23. Thomson RC, Yaszemski MJ, Powers JM, Mikos AG. *Biomaterials*. 1998; 19:1935. [PubMed: 9863527]
24. Rezwan K, Chen QZ, Blaker JJ, Boccaccini AR. *Biomaterials*. 2006; 27:3413. [PubMed: 16504284]
25. Neuendorf RE, Saiz E, Tomsia AP, Ritchie RO. *Acta Biomater*. 2008; 4:1288. [PubMed: 18485842] Russias J, Saiz E, Nalla RK, Tomsia AP. *J Mater Sci*. 2006; 41:5127.
26. Jones JR. *Acta Biomater*. 2013; 9:4457. [PubMed: 22922331]
27. Petite H, Viateau V, Bensaid W, Meunier A, de Pollak C, Bourguignon M, Oudina K, Sedel L, Guillemin G. *Nat Biotechnol*. 2000; 18:959. [PubMed: 10973216]
28. Cancedda R, Giannoni P, Mastrogiamomo M. *Biomaterials*. 2007; 28:4240. [PubMed: 17644173]
29. Gibson I, Best S, Bonfield W. *J Biomed Mater Res*. 1999; 44:422. [PubMed: 10397946] Hing KA, Revell PA, Smith N, Buckland T. *Biomaterials*. 2006; 27:5014. [PubMed: 16790272] Patel N, Best

- SM, Bonfield W, Gibson IR, Hing KA, Damien E, Revell PA. *J Mater Sci Mater Med.* 2002; 13:1199. [PubMed: 15348666]
30. LeGeros RZ. *Clin Mater.* 1993; 14:65. [PubMed: 10171998]
31. Verron E, Khairoun I, Guicheux J, Bouler J-M. *Drug Discovery Today.* 2010; 15:547. [PubMed: 20546919] Bose S, Tarafder S. *Acta Biomater.* 2011
32. Hench LL. *J Am Ceram Soc.* 1998; 81:1705.
33. Rahaman MN, Day DE, Bal BS, Fu Q, Jung SB, Bonewald LF, Tomsia AP. *Acta Biomater.* 2011; 7:2355. [PubMed: 21421084]
34. Fu Q, Saiz E, Rahaman MN, Tomsia AP. *Mater Sci Eng C.* 2011; 31:1245.
35. Hench LL, Polak JM. *Science.* 2002; 295:1014. [PubMed: 11834817]
36. Hench LL, Splinter WC, Allen WC, Greenlee TK, Biomed J. Mater. Res. Symp. 1971; 2:117.
37. Rahaman MN, Brown RF, Bal BS, Day DE. *Semi Arthrop.* 2006; 17:102.
38. Yunos DM, Bretcanu O, Boccaccini AR. *J Mater Sci.* 2008; 43:4433.
39. Jones JR, Hench LL. *J Mater Sci.* 2003; 38:3783. Jones JR, Ahir S, Hench LL. *J Sol-Gel Sci Techn.* 2004; 29:179. Gough JE, Jones JR, Hench LL. *Biomaterials.* 2004; 25:2039. [PubMed: 14741618] Jones JR, Ehrenfried LM, Hench LL. *Biomaterials.* 2006; 27:964. [PubMed: 16102812] Rainer A, Giannitelli SM, Abbruzzese F, Traversa E, Licoccia S, Trombetta M. *Acta Biomater.* 2008; 4:362. [PubMed: 17920344]
40. Chen QZZ, Thompson ID, Boccaccini AR. *Biomaterials.* 2006; 27:2414. [PubMed: 16336997]
41. Vitale-Brovarone C, Verne E, Robiglio L, Appendino P, Bassi F, Martinasso G, Muzio G, Canuto R. *Acta Biomater.* 2007; 3:199. [PubMed: 17085090] Fu Q, Rahaman MN, Bal BS, Brown RF, Day DE. *Acta Biomater.* 2008; 4:1854. [PubMed: 18519173] Vitale-Brovarone C, Baino F, Verne E. *J Mater Sci Mater Med.* 2009; 20:643. [PubMed: 18941868] Fu HL, Fu Q, Zhou N, Huang WH, Rahaman MN, Wang DP, Liu X. *Mat Sci Eng C.* 2009; 29:2275. Liu X, Huang W, Fu H, Yao A, Wang D, Pan H, Lu WW. *J Mater Sci Mater Med.* 2009; 20:365. [PubMed: 18807266] Renghini C, Komlev V, Fiori F, Verne E, Baino F, Vitale-Brovarone C. *Acta Biomater.* 2009; 5:1328. [PubMed: 19038589] Xia W, Chang J. *J Biomed Mater Res B.* 2010; 95:449.
42. Chen QZ, Efthymiou A, Salih V, Boccaccinil AR. *J Biomed Mater Res A.* 2008; 84:1049. [PubMed: 17685403]
43. Liu X, Huang W, Fu H, Yao A, Wang D, Pan H, Lu WW, Jiang X, Zhang X. *J Mater Sci Mater Med.* 2009; 20:1237. [PubMed: 19184371] Liu X, Pan HB, Fu HL, Fu Q, Rahaman MN, Huang WH. *Biomed Mater.* 2010; 5:Oliveira JM, Silva SS, Malafaya PB, Rodrigues MT, Kotobuki N, Hirose M, Gomes ME, Mano JF, Ohgushi H, Reis RL. *J Biomed Mater Res A.* 2009; 91:175. [PubMed: 18780358] Li X, Wang X, Chen H, Jiang P, Dong X, Shi J. *Chem Mater.* 2007; 19:4322.
44. Fu Q, Rahaman MN, Fu HL, Liu X. *J Biomed Mater Res A.* 2010; 95:164. [PubMed: 20544804]
45. Fu QA, Rahaman MN, Bal BS, Bonewald LF, Kuroki K, Brown RF. *J Biomed Mater Res A.* 2010; 95:172. [PubMed: 20540099]
46. Cai S, Xu GH, Yu XZ, Zhang WJ, Xiao ZY, Yao KD. *J Mater Sci Mater Med.* 2009; 20:351. [PubMed: 18807260] Jun IK, Song JH, Choi WY, Koh YH, Kim HE. *J Am Ceram Soc.* 2007; 90:2703. Kim HW, Knowles JC, Kim HE. *J Biomed Mater Res.* 2004; 70:240. Kim HW, Knowles JC, Kim HE. *Biomaterials.* 2004; 25:1279. [PubMed: 14643602] Miao XG, Tan DM, Li J, Xiao Y, Crawford R. *Acta Biomater.* 2008; 4:638. [PubMed: 18054297] Ramay HR, Zhang MQ. *Biomaterials.* 2003; 24:3293. [PubMed: 12763457] Ramay HRR, Zhang M. *Biomaterials.* 2004; 25:5171. [PubMed: 15109841] Wakae H, Takeuchi A, Udo K, Matsuya S, Munar ML, LeGeros RZ, Nakasima A, Ishikawa K. *J Biomed Mater Res A.* 2008; 87:957. [PubMed: 18257056] Xue WC, Bandyopadhyay A, Bose S. *J Biomed Mater Res B.* 2009; 91:831. Zhao J, Duan K, Zhang JW, Lu X, Weng J. *Appl Surf Sci.* 2010; 256:4586.
47. Swain SK, Bhattacharyya S, Sarkar D. *Mat Sci Eng C.* 2011; 31:1240.
48. Almirall A, Larrecq G, Delgado JA, Martinez S, Planell JA, Ginebra MP. *Biomaterials.* 2004; 25:3671. [PubMed: 15020142]
49. Chen GX, Li WW, Zhao BX, Sun K. *J Am Ceram Soc.* 2009; 92:945. Cyster LA, Grant DM, Howdle SM, Rose FRAJ, Irvine DJ, Freeman D, Scotchford CA, Shakesheff KM. *Biomaterials.* 2005; 26:697. [PubMed: 15350773] Huan ZG, Chang J, Zhou J. *J Mater Sci.* 2010; 45:961. Jamuna-Thevi K, Zakaria FA, Othman R, Muhamad S. *Mat Sci Eng C.* 2009; 29:1732. Li

- B, Chen XN, Guo B, Wang XL, Fan HS, Zhang XD. *Acta Biomater*. 2009; 5:134. [PubMed: 18799376] Montufar EB, Traykova T, Gil C, Harr I, Almirall A, Aguirre A, Engel E, Planell JA, Ginebra MP. *Acta Biomater*. 2010; 6:876. [PubMed: 19835998]
50. Yuan HP, de Brujin JD, Zhang XD, van Blitterswijk CA, de Groot K. *J Biomed Mater Res*. 2001; 58:270. [PubMed: 11319740] Sepulveda P, Binner J, Rogero S, Higa O, Bressiani J. *J Biomed Mater Res*. 2000; 50:27. [PubMed: 10644960] Wu ZY, Hill RG, Yue S, Nightingale D, Lee PD, Jones JR. *Acta Biomater*. 2011; 7:1807. [PubMed: 21130188]
51. Vitale-Brovarone C, Di Nunzio S, Bretcanu O, Verne E. *J Mater Sci Mater Med*. 2004; 15:209. [PubMed: 15334992] Liang W, Rahaman MN, Day DE, Marion NW, Riley GC, Mao JJ. *J Non-Cryst Solids*. 2008; 354:1690. Vitale-Brovarone C, Verne E, Robiglio L, Martinasso G, Canuto RA, Muzio G. *J Mater Sci Mater Med*. 2008; 19:471. [PubMed: 17607523] Haimi S, Gorianc G, Moimas L, Lindroos B, Huhtala H, Raty S, Kuokkanen H, Sandor GK, Schmid C, Miettinen S, Suuronen R. *Acta Biomater*. 2009; 5:3122. [PubMed: 19428318]
52. Brovarone CV, Verne E, Appendino P. *J Mater Sci Mater Med*. 2006; 17:1069. [PubMed: 17122921] Fu Q, Rahaman MN, Bal BS, Huang W, Day DE. *J Biomed Mater Res A*. 2007; 82:222. [PubMed: 17266021] Brown RF, Day DE, Day TE, Jung S, Rahaman MN, Fu Q. *Acta Biomater*. 2008; 4:387. [PubMed: 17768097] Zhang H, Ye XJ, Li JS. *Biomed Mater*. 2009; 4Baino F, Verne E, Vitale-Brovarone C. *Mat Sci Eng C*. 2009; 29:2055. Wu SC, Hsu HC, Hsiao SH, Ho WF. *J Mater Sci Mater Med*. 2009; 20:1229. [PubMed: 19160020] Bellucci D, Cannillo V, Ciardelli G, Gentile P, Sola A. *Ceram Int*. 2010; 36:2449.
53. Yao XM, Tan SH, Jiang DL. *J Mater Sci*. 2005; 40:4939.
54. Isobe T, Tomita T, Kameshima Y, Nakajima A, Okada K. *J Eur Ceram Soc*. 2006; 26:957. Isobe T, Karneshima Y, Nakajima A, Okada K, Hotta Y. *J Porous Mat*. 2006; 13:269. Isobe T, Kameshima Y, Nakajima A, Okada K. *J Eur Ceram Soc*. 2007; 27:61.
55. Zhang GJ, Yang JF, Ohji T. *J Am Ceram Soc*. 2001; 84:1395.
56. Nakahira A, Nishimura F, Kato S, Iwata M, Takeda S. *J Am Ceram Soc*. 2003; 86:1230.
57. Ota T, Takahashi M, Hibi T, Ozawa M, Suzuki S, Hikichi Y, Suzuki H. *J Am Ceram Soc*. 1995; 78:3409. Ota T, Imaeda M, Takase H, Kobayashi M, Kinoshita N, Hirashita T, Miyazaki H, Hikichi Y. *J Am Ceram Soc*. 2000; 83:1521. Greil P. *J Eur Ceram Soc*. 2001; 21:105. Rambo CR, Sieber H. *Adv Mater*. 2005; 17:1088. Colombo P, Philos T R Soc A. 2006; 364:109.
58. Miyagawa N, Shinohara N. *J Ceram Soc Jpn*. 1999; 107:673.
59. Schoof H, Apel J, Heschel I, Rau G. *J Biomed Mater Res*. 2001; 58:352. [PubMed: 11410892] Zhang HF, Hussain I, Brust M, Butler MF, Rannard SP, Cooper AI. *Nat Mater*. 2005; 4:787. [PubMed: 16184171] Song JH, Koh YH, Kim HE, Li LH, Bahn HJ. *J Am Ceram Soc*. 2006; 89:2649. Wegst UGK, Schechter M, Donius AE, Hunger PM. *Philos T R Soc A*. 2010; 368:2099.
60. Deville S, Saiz E, Nalla RK, Tomsia AP. *Science*. 2006; 311:515. [PubMed: 16439659] Fu Q, Rahaman MN, Dogan F, Bal BS. *J Biomed Mater Res B*. 2008; 86B:125. Liu X, Rahaman MN, Fu QA. *Acta Biomater*. 2011; 7:406. [PubMed: 20807594]
61. Fu Q, Rahaman MN, Dogan F, Bal BS. *J Biomed Mater Res B*. 2008; 86:514.
62. Fu Q, Rahaman MN, Bal BS, Brown RF. *J Biomed Mater Res A*. 2010; 93:1380. [PubMed: 19911380]
63. Deville S, Saiz E, Tomsia AP. *Biomaterials*. 2006; 27:5480. [PubMed: 16857254]
64. Sachlos E, Czernuszka JT. *Eur Cells Mater*. 2003; 3:29. Chu, T-MG. *Scaffolding in Tissue Engineering*. Ma, X., Eliseeff, J., editors. Vol. 139. Marcel Dekker, Inc.; 2005. Miranda P, Saiz E, Grynn K, Tomsia AP. *Acta Biomater*. 2006; 2:457. [PubMed: 16723287] Russias J, Saiz E, Deville S, Grynn K, Liu G, Nalla RK, Tomsia AP. *J Biomed Mater Res A*. 2007; 83:434. [PubMed: 17465019] Franco J, Hunger P, Launey ME, Tomsia AP, Saiz E. *Acta Biomater*. 2010; 6:218. [PubMed: 19563923] Huang TS, Rahaman MN, Doiphode ND, Leu MC, Bal BS, Day DE. *Mater Sci Eng C*. 2011; 31:1482. Derby B. *Science*. 2012; 338:921. [PubMed: 23161993] Miller JS, Stevens KR, Yang MT, Baker BM, Nguyen DHT, Cohen DM, Toro E, Chen AA, Galie PA, Yu X, Chaturvedi R, Bhatia SN, Chen CS. *Nat Mater*. 2012; 11:768. [PubMed: 22751181]
65. Miranda P, Pajares A, Saiz E, Tomsia AP, Guiberteau F. *J Biomed Mater Res A*. 2008; 85:218. [PubMed: 17688280]
66. Fu Q, Saiz E, Tomsia AP. *Adv Funct Mater*. 2011; 21:1058. [PubMed: 21544222]

67. Goodridge RD, Wood DJ, Ohtsuki C, Dalgarno KW. *Acta Biomater*. 2007; 3:221. [PubMed: 17215172]
68. Deliormanli AM, Rahaman MN. *J Eur Ceram Soc*. 2012; 32:3637.
69. ASTM International, Vol. C1424-10. ASTM International; West Conshohocken, PA: 2010.
70. Jun IK, Koh YH, Kim HE. *J Am Ceram Soc*. 2006; 89:391.
71. Barralet JE, Grover L, Gaunt T, Wright AJ, Gibson IR. *Biomaterials*. 2002; 23:3063. [PubMed: 12102177] Barralet JE, Gaunt T, Wright AJ, Gibson IR, Knowles JC. *J Biomed Mater Res*. 2002; 63:1. [PubMed: 11787022] Rice RW. *J Mater Sci*. 1993; 28:2187. Liu DM. *J Mater Sci Lett*. 1996; 15:419.
72. Rossi RC. *J Am Ceram Soc*. 1968; 51:433.
73. Rice RW. *J Am Ceram Soc*. 1993; 76:1801.
74. Watchman, JB., Canon, WR., Mattewson, MJ. Mechanical properties of ceramics. John Wiley & Sons; Hoboken, NJ: 2009.
75. Gibson, LJ., Ashby, MF. Cellular solids : structure and properties. Cambridge University Press; Cambridge; New York: 1997.
76. Pirhonen E, Niiranen H, Niemela T, Brink M, Tormala P. *J Biomed Mater Res B*. 2006; 77:227.
77. De Diego MA, Coleman NJ, Hench LL. *J Biomed Mater Res*. 2000; 53:199. [PubMed: 10813757]
78. Ginebra MP, Delgado JA, Harr I, Almirall A, Del Valle S, Planell JA. *J Biomed Mater Res A*. 2007; 80:351. [PubMed: 17001653] Guo DG, Xu KW, Han Y. *J Biomed Mater Res A*. 2009; 88:43. [PubMed: 18257062] Landi E, Valentini F, Tampieri A. *Acta Biomaterialia*. 2008; 4:1620. [PubMed: 18579459] Macchetta A, Turner IG, Bowen CR. *Acta Biomater*. 2009; 5:1319. [PubMed: 19112055] Gupta G, El-Ghannam A, Kirakodu S, Khraisheh M, Zbib H. *J Biomed Mater Res B*. 2007; 81:387. Galea LG, Bohner M, Lemaitre J, Kohler T, Muller R. *Biomaterials*. 2008; 29:3400. [PubMed: 18495242] Ren J, Zhao P, Ren TB, Gu SY, Pan KF. *J Mater Sci Mater Med*. 2008; 19:1075. [PubMed: 17701303] Zhang FM, Lin KL, Chang J, Lu JX, Ning CQ. *J Eur Ceram Soc*. 2008; 28:539. Descamps M, Richart O, Hardouin P, Hornez JC, Leriche A. *Ceram Int*. 2008; 34:1131. Liu YX, Kim JH, Young D, Kim S, Nishimoto SK, Yang YZ. *J Biomed Mater Res A*. 2010; 92:997. [PubMed: 19296544] Lin KL, Chen L, Qu HY, Lu JX, Chang J. *Ceram Int*. 2011; 37:2397. Ribeiro GBM, Trommer RM, dos Santos LA, Bergmann CP. *Mater Lett*. 2011; 65:275. Chu TMG, Orton DG, Hollister SJ, Feinberg SE, Halloran JW. *Biomaterials*. 2002; 23:1283. [PubMed: 11808536] Li X, Li DC, Lu BH, Wang CT. *J Porous Mat*. 2008; 15:667. Cordell JM, Vogl ML, Johnson AJW. *J Mech Behav Biomed*. 2009; 2:560. Yang HY, Chi XP, Yang S, Evans JRG. *J Mater Sci Mater Med*. 2010; 21:1503. [PubMed: 20145978] Guo DG, Xu KW, Liu YX. *J Mater Sci Mater Med*. 2010; 21:1927. [PubMed: 20217190]
79. Dong J, Kojima H, Uemura T, Kikuchi M, Tateishi T, Tanaka J. *J Biomed Mater Res*. 2001; 57:208. [PubMed: 11484183]
80. Martinez-Vazquez FJ, Perera FH, Miranda P, Pajares A, Guiberteau F. *Acta Biomater*. 2010; 6:4361. [PubMed: 20566307]
81. Xie HX, Wang QB, Ye QS, Wan CX, Li LJ. *J Mater Sci Mater Med*. 2012; 23:1033. [PubMed: 22311075] Soon YM, Shin KH, Koh YH, Lee JH, Kim HE. *Mater Lett*. 2009; 63:1548. Park JH, Bae JY, Shim J, Jeon I. *Mater Charact*. 2012; 71:103. Ebrahimi M, Pripatnanont P, Monmaturapoj N, Suttapreyasri S. *J Biomed Mater Res A*. 2012; 100:2260. [PubMed: 22499354] Soon YM, Shin KH, Koh YH, Lee JH, Choi WY, Kim HE. *J Eur Ceram Soc*. 2011; 31:13.
82. ASTM International, Vol. C1161-02C. West Conshohocken, Pennsylvania, USA: 2008.
83. Chen QZ, Boccaccini AR. *J Biomed Mater Res A*. 2006; 77:445. [PubMed: 16444684]
84. Pernot F, Etienne P, Boschet F, Datas L. *J Am Ceram Soc*. 1999; 82:641.
85. Xu HHK, Simon CG. *Biomaterials*. 2005; 26:1337. [PubMed: 15482821] Xu HHK, Weir MD, Burguera EF, Fraser AM. *Biomaterials*. 2006; 27:4279. [PubMed: 16650891] Rodriguez-Lorenzo LM, Vallet-Regi M, Ferreira JMF. *J Biomed Mater Res*. 2002; 60:232. [PubMed: 11857429]
86. Mellor M, Hawkes I. *Engineering Geology*. 1971; 5:173.
87. Ding SJ, Wang CW, Chen DCH, Chang HC. *Ceram Int*. 2005; 31:691.
88. Charriere E, Lemaitre J, Zysset P. *Biomaterials*. 2003; 24:809. [PubMed: 12485799] Takagi S, Chow LC. *J Mater Sci Mater Med*. 2001; 12:135. [PubMed: 15348319]

89. ASTM International, Vol. C1239-07. West Conshohocken, Pennsylvania, USA: 2007.
90. Weibull W. *J Appl Mech-T ASME*. 1951; 18:293.
91. Bergman B. *J Mater Sci Lett*. 1984; 3:689.Sullivan JD, Lauzon PH. *J Mater Sci Lett*. 1986; 5:1245.
92. Fan X, Case ED, Ren F, Shu Y, Baumann MJ. *J Mech Behav Biomed*. 2012; 8:99.Fan X, Case ED, Ren F, Shu Y, Baumann MJ. *J Mech Behav Biomed*. 2012; 8:21.
93. Genet M, Houmard M, Eslava S, Saiz E, Tomsia AP. *J Eur Ceram Soc*. 2012
94. Chan KS, Liang W, Francis WL, Nicolella DP. *J Mech Behav Biomed*. 2010; 3:584.Miranda P, Pajares A, Guiberteau F. *Acta Biomater*. 2008; 4:1715. [PubMed: 18583207]
95. Miranda P, Pajares A, Saiz E, Tomsia AP, Guiberteau F. *J Biomed Mater Res A*. 2007; 83:646. [PubMed: 17508415]
96. Sanchez-Palencia E. *International Journal of Engineering Science*. 1974; 12:331.
97. Ritchie RO. *Nat Mater*. 2011; 10:817. [PubMed: 22020005]
98. Green, DJ. An introduction to the mechanical properties of ceramics. University Press; Cambridge: 1998.
99. Ashby, MF. Materials selection in mechanical design. Pergamon; 1992. Demetriou MD, Launey ME, Garrett G, Schramm JP, Hofmann DC, Johnson WL, Ritchie RO. *Nat Mater*. 2011; 10:123. [PubMed: 21217693]
100. Demetriou MD, Veazey C, Harmon JS, Schramm JP, Johnson WL. *Phys Rev Lett*. 2008; 101:Axinte E. *Mater Design*. 2012; 35:518.
101. Demetriou MD, Wiest A, Hofmann DC, Johnson WL, Han B, Wolfson N, Wang GY, Liaw PK. *JOM*. 2010; 62:83.
102. Davidge, RW. Mechanical behaviour of ceramics. Cambridge University Press; Cambridge; New York: 1979. Sakai M, Bradt RC. *Int Mater Rev*. 1993; 38:53.
103. Becher PF. *J Am Ceram Soc*. 1991; 74:255.
104. ASTM International, Vol. ASTM C1421-10. West Conshohocken, Pennsylvania, USA: 2010.
105. Maiti SK, Ashby MF, Gibson LJ. *Scripta Metall Mater*. 1984; 18:213.Huang JS, Gibson LJ. *Acta Metall Mater*. 1991; 39:1627.
106. Quintana-Alonso I, Mai SP, Fleck NA, Oakes DCH, Twigg MV. *Acta Mater*. 2010; 58:201.
107. Deng ZY, She JH, Inagaki Y, Yang JF, Ohji T, Tanaka Y. *J Eur Ceram Soc*. 2004; 24:2055.
108. Brezny R, Green DJ. *J Am Ceram Soc*. 1989; 72:1145.
109. Shyam A, Lara-Curcio E, Watkins TR, Parten RJ. *J Am Ceram Soc*. 2008; 91:1995.
110. Barinov SM, Sakai M. *J Mater Res*. 1994; 9:1412.
111. Peroglio M, Gremillard L, Gauthier C, Chazeau L, Verrier S, Alini M, Chevalier J. *Acta Biomaterialia*. 2010; 6:4369. [PubMed: 20553981] Peroglio M, Gremillard L, Chevalier J, Chazeau L, Gauthier C, Hamaide T. *J Eur Ceram Soc*. 2007; 27:2679.
112. Bretcanu O, Misra S, Roy I, Renghini C, Fiori F, Boccaccini AR, Salih V. *J Tissue Eng Regen M*. 2009; 3:139. [PubMed: 19170250]
113. Freeman MAR, Todd RC, Pirie CJ. *J Bone Joint Surg Br*. 1974; B 56:698.Riggs BL, Melton LJ. *Bone*. 1995; 17:S505.
114. Daffner RH, Pavlov H. *Am J Roentgenol*. 1992; 159:245. [PubMed: 1632335] Silva MJ, Keaveny TM, Hayes WC. *Spine*. 1997; 22:140. [PubMed: 9122793]
115. Evans AG. *Int J Fracture*. 1980; 16:485.
116. Ritchie RO, Dauskardt RH. *Nippon Seram Kyo Gak*. 1991; 99:1047.
117. ASTM International, Vol. C1576-05. West Conshohocken, Pennsylvania, USA: 2010. ASTM International, Vol. C1368-10. West Conshohocken, Pennsylvania, USA: 2011.
118. Benaqqa C, Chevalier J, Saadaoui M, Fantozzi G. *Biomaterials*. 2005; 26:6106. [PubMed: 15890401]
119. Shu YT, Case ED, Baumann M. *J Mater Sci*. 2012; 47:6542.Barinov SM, Malkov MA. *J Mater Sci Lett*. 1993; 12:1039.Troczyński TB, Nicholson PS. *J Am Ceram Soc*. 1990; 73:164.Kokubo T, Ito S, Shigematsu M, Sanka S, Yamamoto T. *J Mater Sci*. 1987; 22:4067.Case ED, Smith IO, Baumann MJ. *Mat Sci Eng A*. 2005; 390:246.
120. Barinov SM, Shevchenko VY. *J Mater Sci Lett*. 1995; 14:582.

121. Raynaud S, Champion E, Bernache-Assolant D, Tetard D. *J Mater Sci Mater Med.* 1998; 9:221.
122. Bloyer DR, McNaney JM, Cannon RM, Saiz E, Tomsia AP, Ritchie RO. *Biomaterials.* 2007; 28:4901. [PubMed: 17714778] Pavon J, Jimenez-Pique E, Anglada M, Lopez-Esteban S, Saiz E, Tomsia AP. *J Eur Ceram Soc.* 2006; 26:1159.
123. Bolz LH. *Wiederho. Sm. J Am Ceram Soc.* 1970; 53:543.
124. Choi K, Goldstein SA. *J Biomech.* 1992; 25:1371. [PubMed: 1491015]
125. Ganguly P, Moore TLA, Gibson LJ. *J Biomech Eng-T ASME.* 2004; 126:330.
126. Paris P, Erdogan F. *J Basic Eng-T ASME.* 1963; 85:528.
127. Bajaj D, Nazari A, Eidelman N, Arola DD. *Biomaterials.* 2008; 29:4847. [PubMed: 18804277]
128. Peterlik H, Roschger P, Klaushofer K, Fratzl P. *Nat Mater.* 2006; 5:52. [PubMed: 16341218]  
Meyers MA, Chen PY, Lin AYM, Seki Y. *Prog Mater Sci.* 2008; 53:1.Tang ZY, Kotov NA, Magonov S, Ozturk B. *Nat Mater.* 2003; 2:413. [PubMed: 12764359] Fratzl P, Weinkamer R. *Prog Mater Sci.* 2007; 52:1263.
129. Evans AG. *J Am Ceram Soc.* 1990; 73:187.
130. Kokubo T. *Biomaterials.* 1991; 12:155. [PubMed: 1878450]
131. Kokubo T, Ito S, Shigematsu M, Sakka S, Yamamoto T. *J Mater Sci.* 1985; 20:2001.
132. Apel E, Deubener J, Bernard A, Holand M, Muller R, Kappert H, Rheinberger V, Holand W. *J Mech Behav Biomed.* 2008; 1:313.
133. Amaral M, Lopes MA, Silva RF, Santos JD. *Biomaterials.* 2002; 23:857. [PubMed: 11771704]  
Liu DM, Chou HM. *J Mater Sci-Mater M.* 1994; 5:7.Ryu HS, Lee JK, Seo JH, Kim H, Hong KS, Kim DJ, Lee JH, Lee DH, Chang BS, Lee CK, Chung SS. *J Biomed Mater Res A.* 2004; 68A: 79.Marghussian VK, Mesgar ASM. *Ceram Int.* 2000; 26:415.Kanchanarat N, Bandyopadhyay-Ghosh S, Reaney IM, Brook IM, Hatton PV. *J Mater Sci.* 2008; 43:759.Thompson ID, Hench LL. *P I Mech Eng H.* 1998; 212:127.Rahaman MN, Yao AH, Bal BS, Garino JP, Ries MD. *J Am Ceram Soc.* 2007; 90:1965.
134. Clupper DC, Hench LL, Mecholsky JJ. *J Eur Ceram Soc.* 2004; 24:2929.
135. Mantzos T, Chatzistavrou X, Roether JA, Hupa L, Arstila H, Boccaccini AR. *Biomed Mater.* 2009; 4
136. Mourino V, Newby P, Boccaccini AR. *Adv Eng Mater.* 2010; 12:B283.
137. Sanchez C, Arribart H, Guille MMG. *Nat Mater.* 2005; 4:277. [PubMed: 15875305] Smith BL, Schaffer TE, Viani M, Thompson JB, Frederick NA, Kindt J, Belcher A, Stucky GD, Morse DE, Hansma PK. *Nature.* 1999; 399:761.Mayer G. *Science.* 2005; 310:1144. [PubMed: 16293751]  
Song F, Soh AK, Bai YL. *Biomaterials.* 2003; 24:3623. [PubMed: 12809793]
138. Launey ME, Munch E, Alsem DH, Barth HB, Saiz E, Tomsia AP, Ritchie RO. *Acta Mater.* 2009; 57:2919.Munch E, Launey ME, Alsem DH, Saiz E, Tomsia AP, Ritchie RO. *Science.* 2008; 322:1516. [PubMed: 19056979]
139. Poologasundarampillai G, Ionescu C, Tsikou O, Murugesan M, Hill RG, Stevens MM, Hanna JV, Smith ME, Jones JR. *J Mater Chem.* 2010; 20:8952.
140. Poologasundarampillai G, Yu B, Tsikou O, Valliant E, Yue S, Lee PD, Hamilton RW, Stevens MM, Kasuga T, Jones JR. *Soft Matter.* 2012; 8:4822.
141. Manzano M, Arcos D, Rodríguez Delgado M, Ruiz E, Gil FJ, Vallet-Regí M. *Chem Mater.* 2006; 18:5696.
142. Yoshikawa H, Tamai N, Murase T, Myoui A. *J R Soc Interface.* 2009; 6:S341. [PubMed: 19106069]
143. Walsh WR, Vizesi F, Michael D, Auld J, Langdown A, Oliver R, Yu Y, Irie H, Bruce W. *Biomaterials.* 2008; 29:266. [PubMed: 18029011]

## Biographies



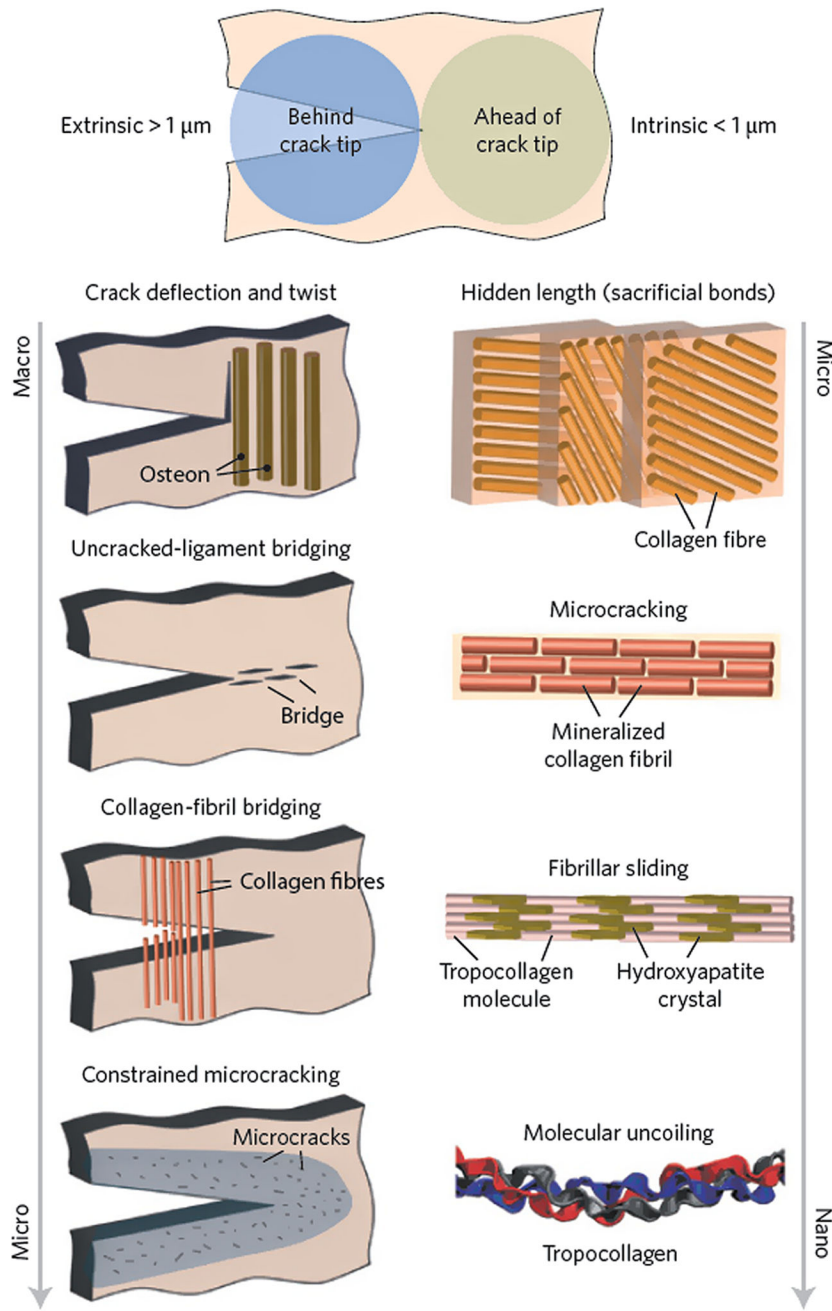
**Qiang Fu** is a Glass Development Scientist at Corning Inc. and a guest scientist at the Lawrence Berkeley National Laboratory. He received his BS and MS in Materials Science from Tongji University (Shanghai, China), and Ph.D. in Ceramic Engineering from Missouri University of Science and Technology in 2009. Fu did his postdoctoral research at the Lawrence Berkeley National Laboratory before joining Corning Inc. in 2011. His research interests include bioactive glass and ceramics, chemically strengthened glass and glass-ceramics, and processing and mechanical properties of porous materials.



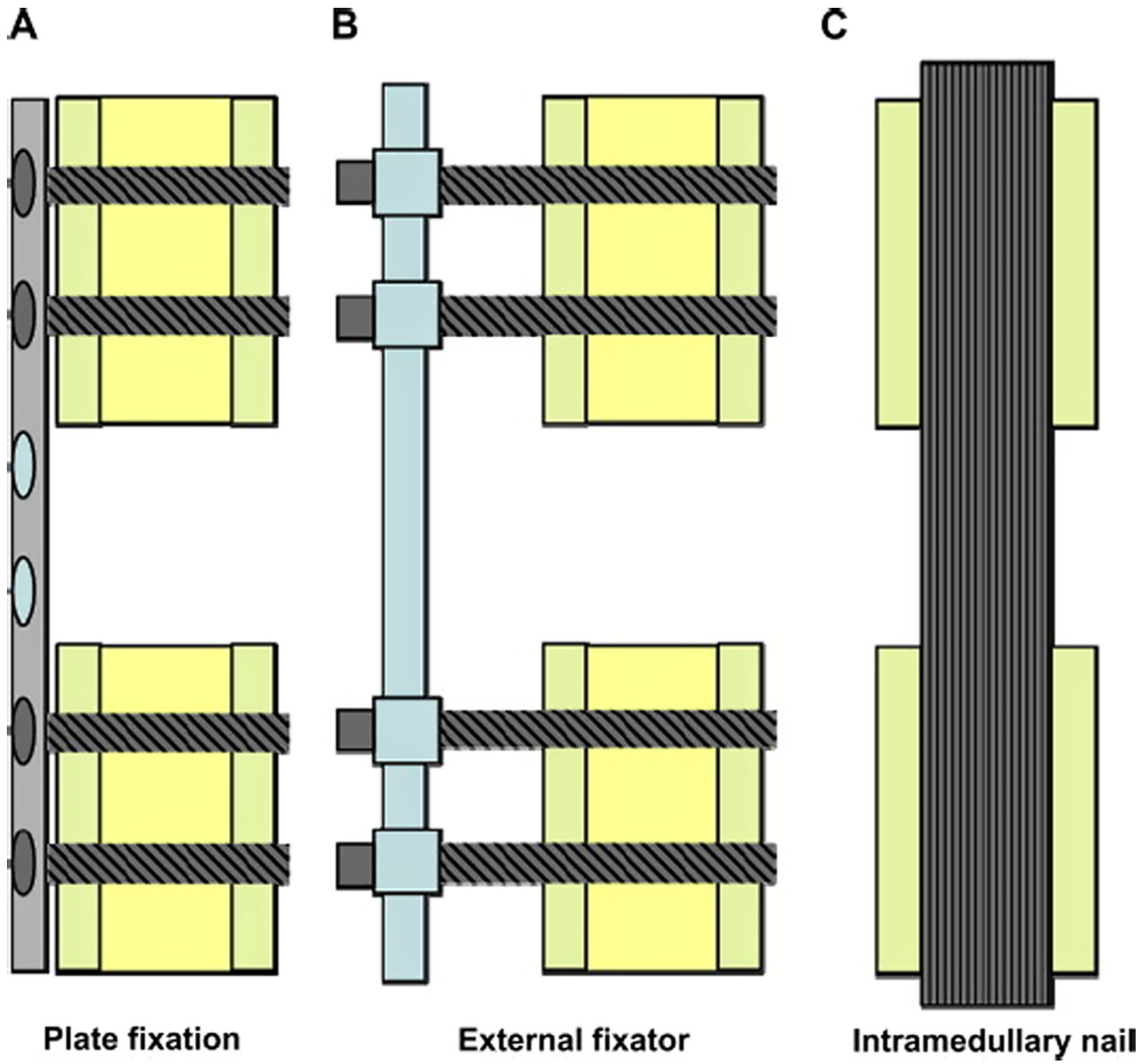
**Mohamed N. Rahaman** is a Professor of Materials Science and Engineering and Director of the Center for Bone and Tissue Repair and Regeneration, Missouri University of Science and Technology (Missouri S&T). Educated at Cambridge University and Sheffield University, England, he was a Research Fellow at Leeds University, England, and a Staff Scientist at the Lawrence Berkeley National Laboratory, Berkeley, California, before joining Missouri S&T in 1986. Dr. Rahaman is a Fellow of the American Ceramic Society and a Member of the Society for Biomaterials. He is the author of four books and the author/co-author of approximately 230 articles, mainly in the areas of advanced ceramics and biomaterials.



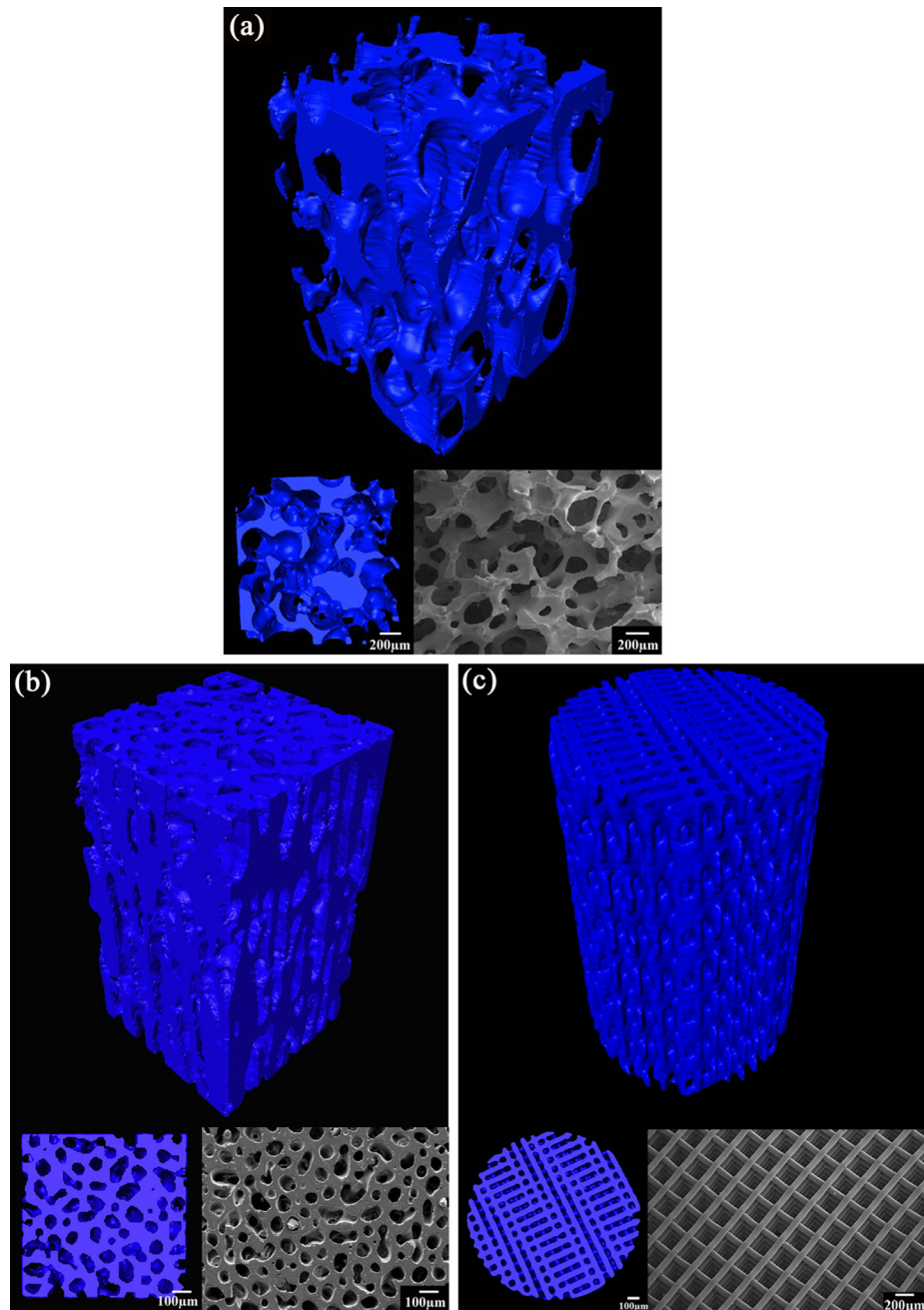
**Antoni P. Tomsia** is a Senior Scientist at the Materials Sciences Division, Lawrence Berkeley National Laboratory. A native of Poland, he received an M.S. from the University of Mining and Metallurgy, Krakow, and an M.S. and Ph.D. from the Institute of Materials Science, also in Krakow. He joined Lawrence Berkeley National Laboratory in 1978. Tomsia has published more than 200 papers in the fields of biomaterials, ceramic-metal joining, and physics of solid-liquid interfaces.



**Figure 1.**  
The prevailing toughening mechanisms in cortical bone.<sup>[14]</sup>

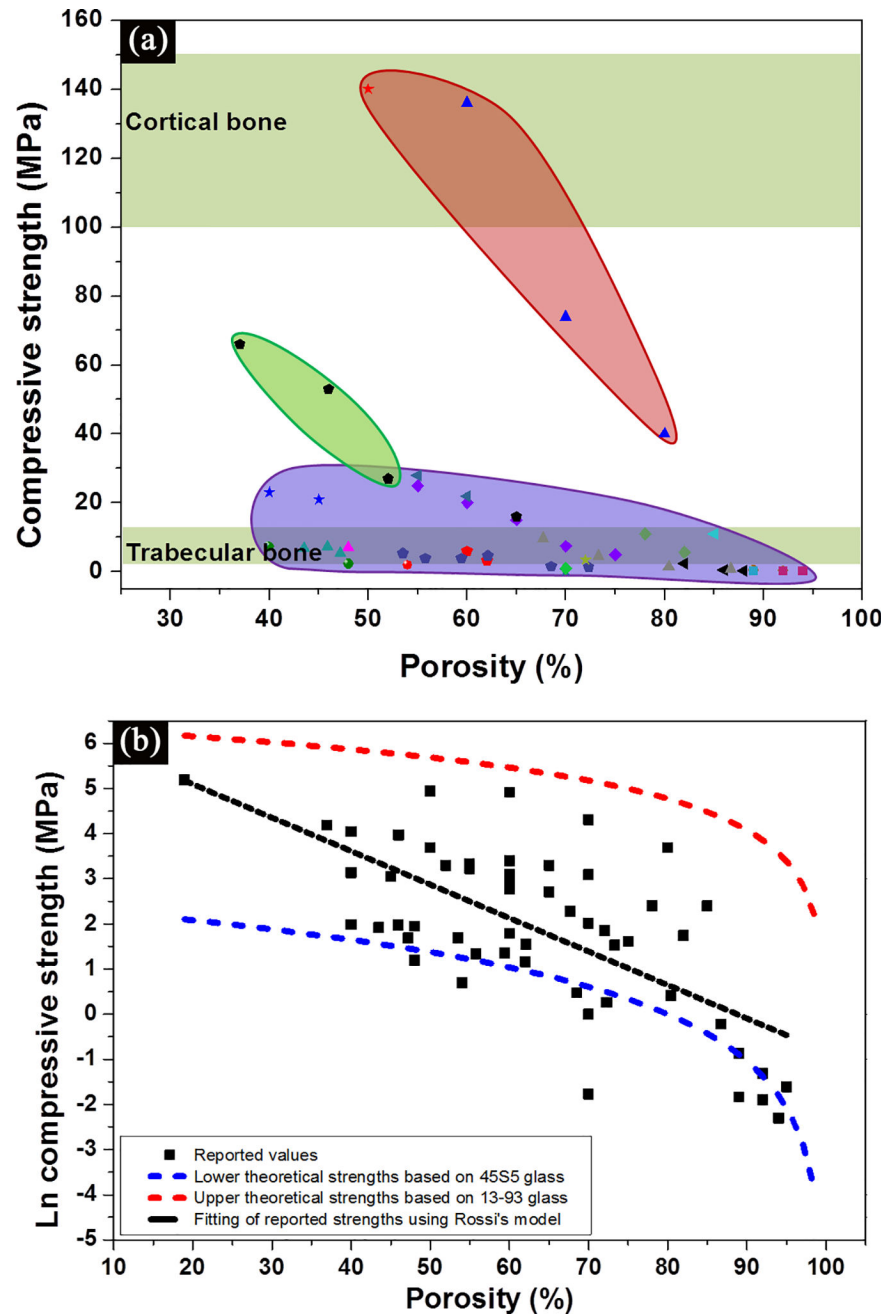


**Figure 2.**  
Schematic representation of commonly applied methods for the fixation of segmental defects in large animal models. A) plate fixation, B) external fixator, and C) intramedullary nail.<sup>[18]</sup>

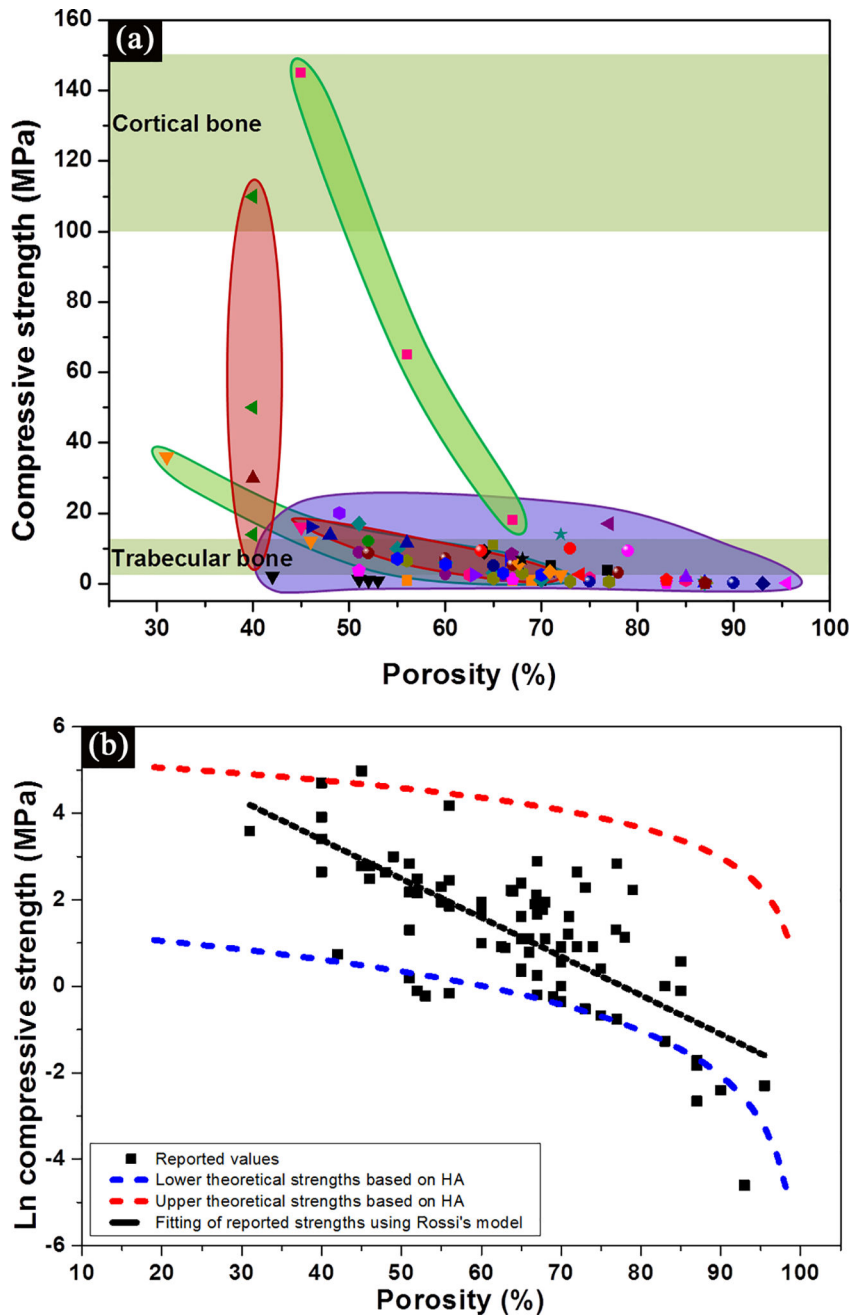


**Figure 3.**

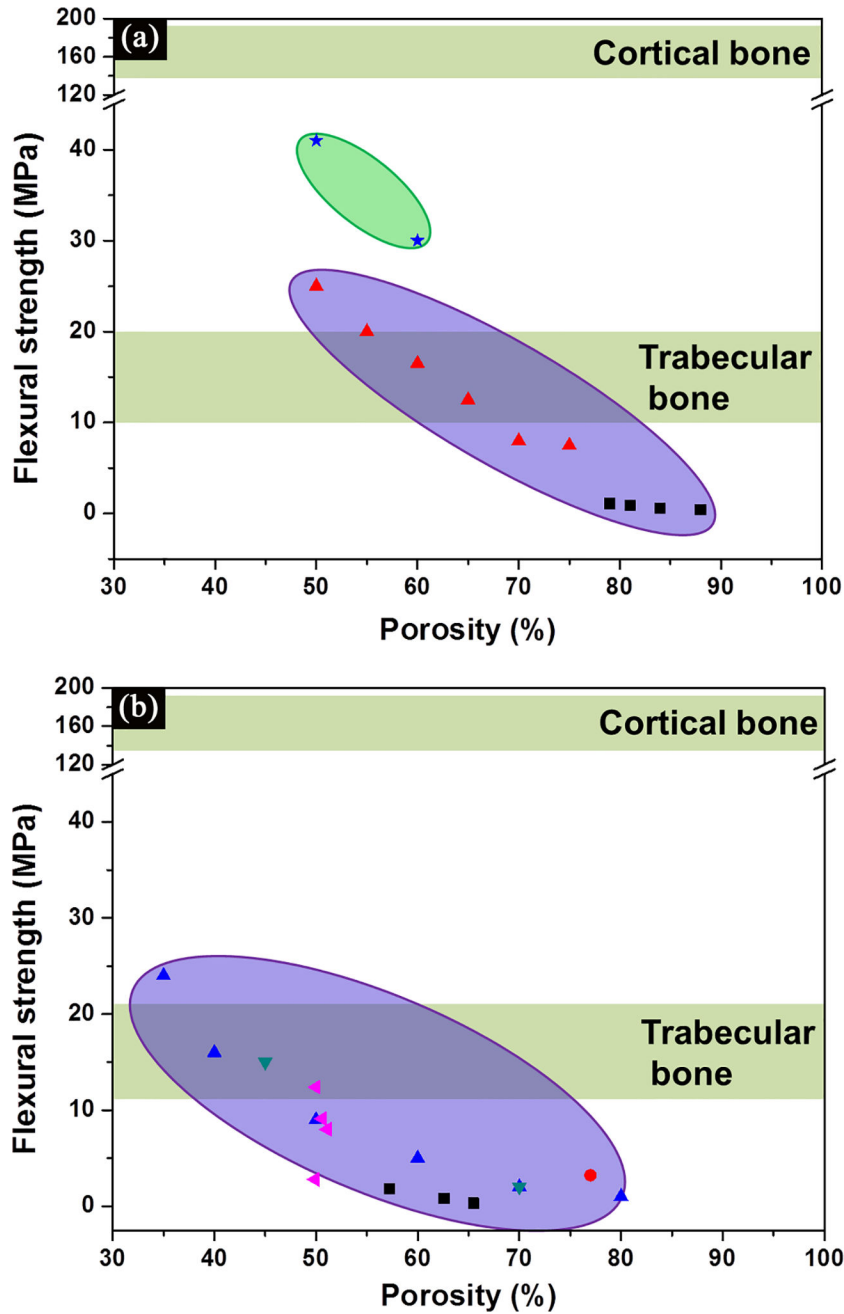
Representative images of bioactive glass 13–93 scaffolds prepared by different techniques: (a) isotropic scaffold by a polymer foam replication technique; (b) anisotropic scaffold prepared by a freeze casting technique; (c) periodic scaffold by a direct-ink writing technique

**Figure 4.**

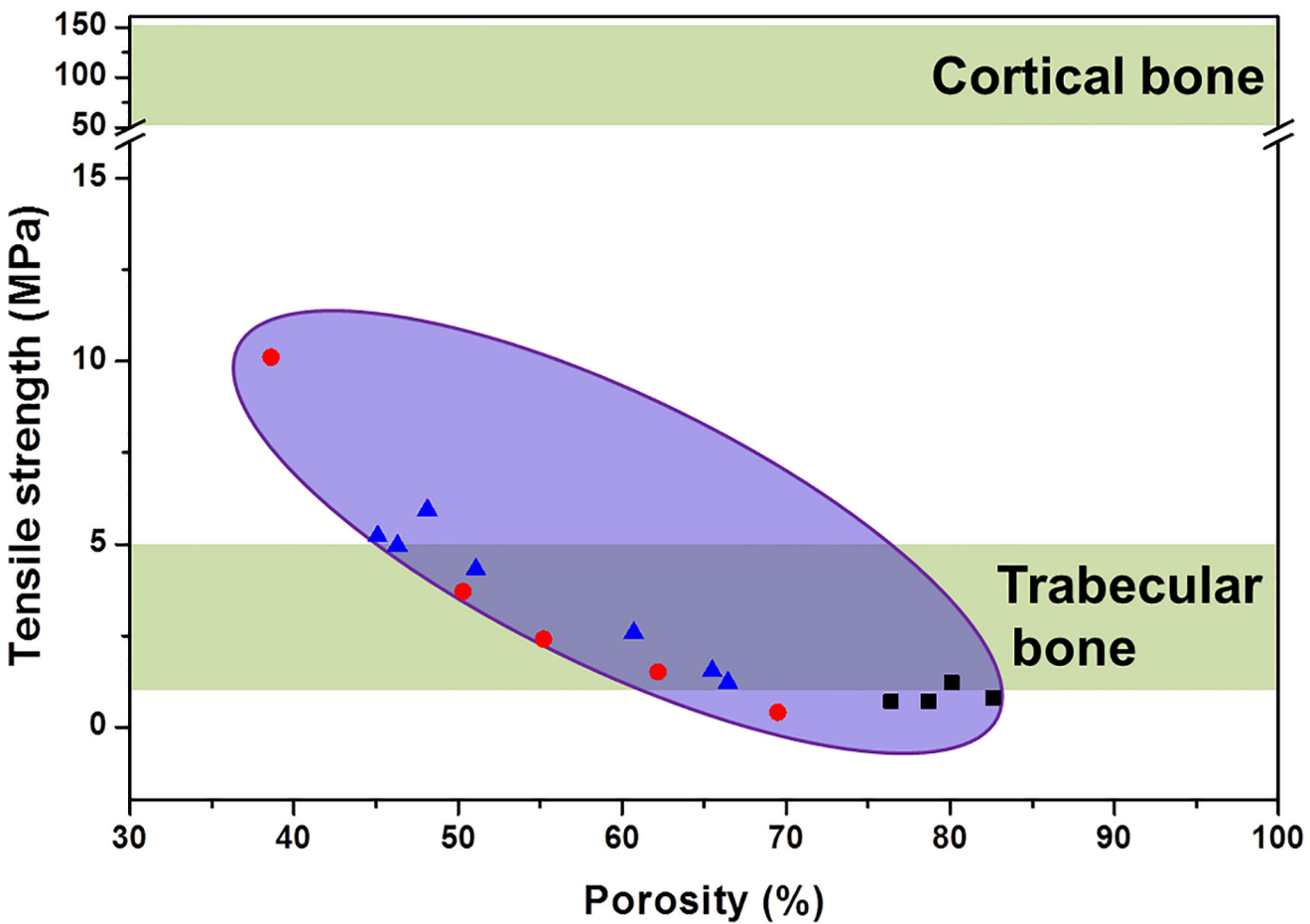
(a) Compressive strength of bioactive glass scaffolds compiled from literature studies, and grouped based on their structures. Purple: isotropic scaffolds; green: anisotropic scaffolds; pink: perodic scaffolds;<sup>[40, 41, 42, 44, 52, 62, 66, 70]</sup> (b) Influence of porosity on the compressive strength of bioactive glass scaffolds. The black dotted line indicates a linear fitting by Rossi model,<sup>[72]</sup> while red and blue dotted lines indicates the upper and lower theoretical strength predicted by Gibson and Ashby model.<sup>[75]</sup>

**Figure 5.**

(a) Compressive strength of bioactive ceramic scaffolds compiled from literature studies, and grouped based on their structures. Purple: isotropic scaffolds; green: anisotropic scaffolds; pink: periodic scaffolds.<sup>[46, 47, 48, 49, 61, 63, 65, 78, 79, 80]</sup> (b) Influence of porosity on the compressive strength of bioactive ceramic scaffolds. The black dotted line indicates a linear fitting by Rossi model<sup>[72]</sup>, while red and blue dotted lines indicate the upper and lower theoretical strength predicted by Gibson and Ashby model.<sup>[75]</sup>

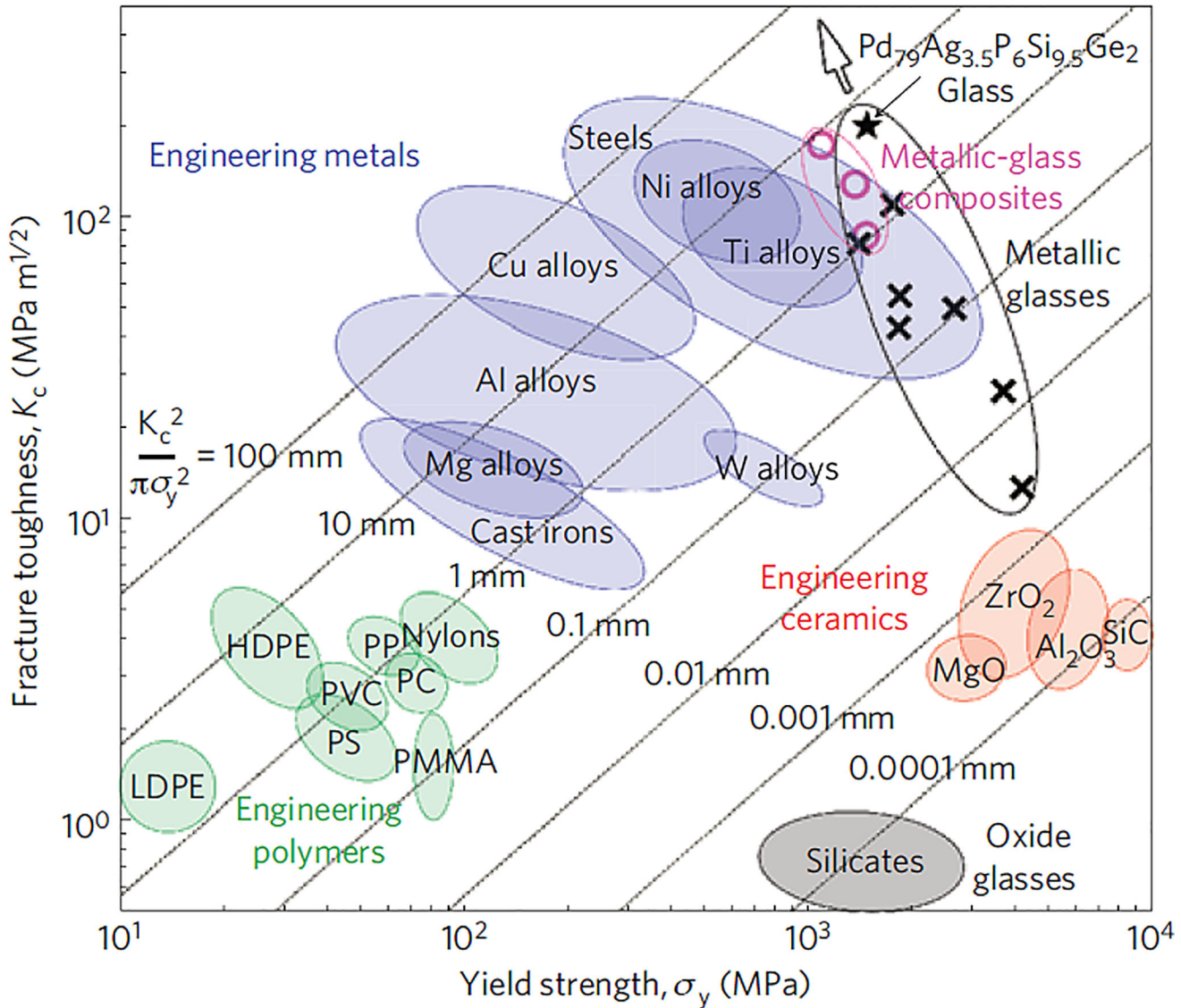
**Figure 6.**

Flexural strength of (a) bioactive glass, and (b) ceramic scaffolds compiled from literature studies, and grouped based on their structures.<sup>[40, 53, 79, 84, 85]</sup> Purple: isotropic scaffolds; pink: peridotic scaffolds.

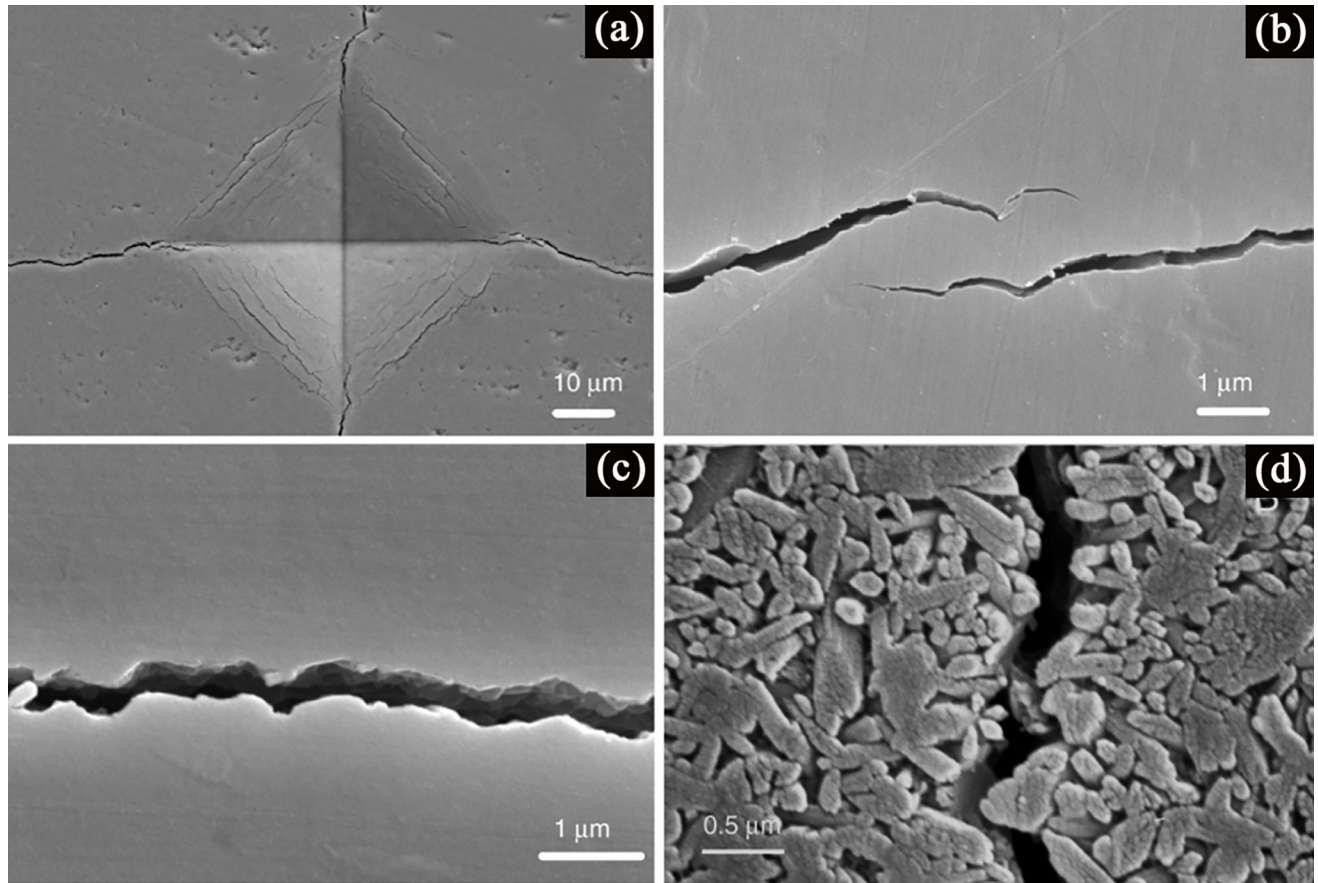


**Figure 7.**

Tensile strength of isotropic bioactive ceramic scaffolds compiled from literature studies.  
[48, 87, 88]

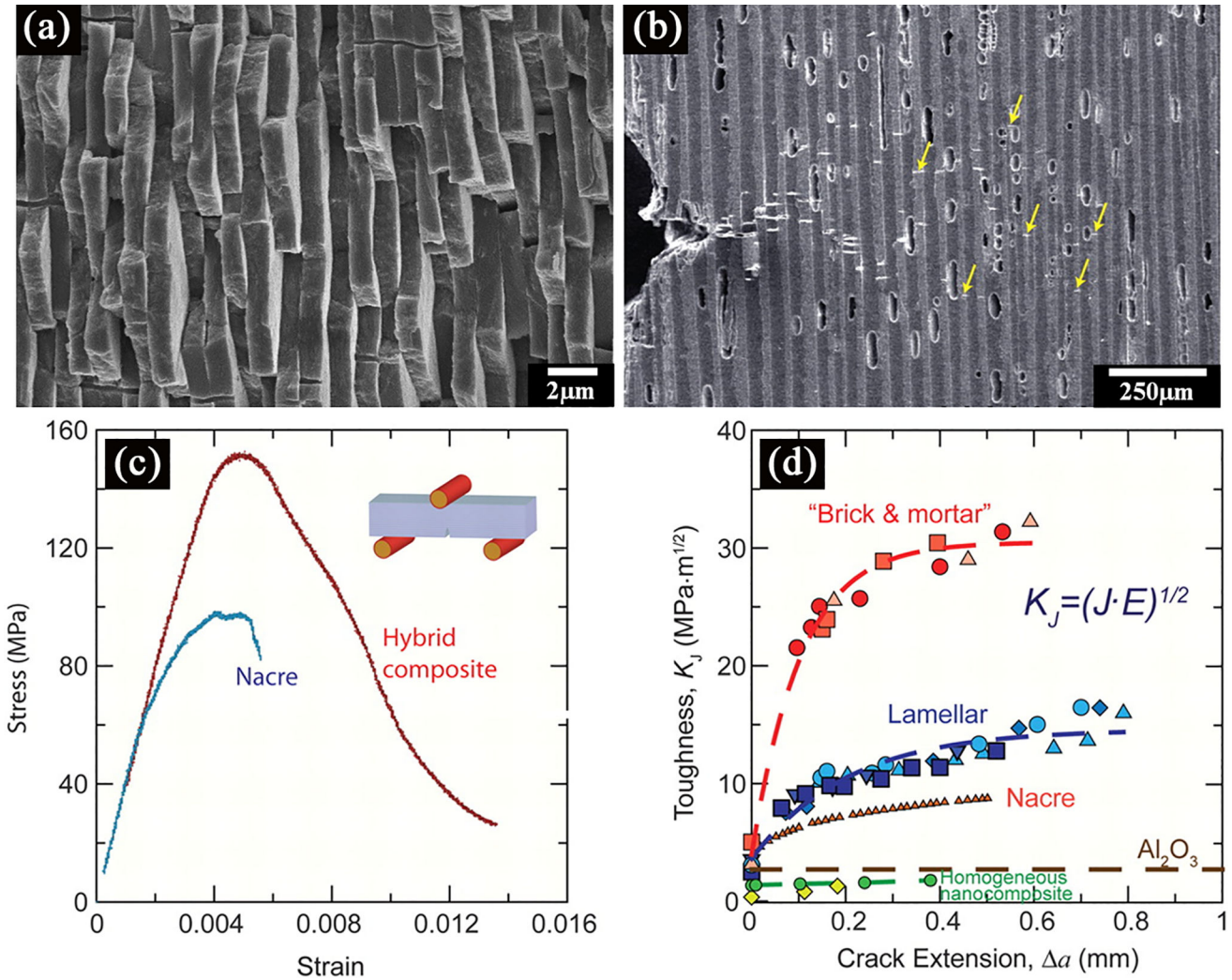
**Figure 8.**

Ashby map of the damage tolerance (toughness versus strength) of materials. Ranges of fracture toughness versus yield strength are shown for oxide glasses, engineering ceramics, engineering polymers, engineering metals and metallic glasses. Yield-strength data shown for oxide glasses and ceramics represent ideal limits.<sup>[99]</sup>



**Figure 9.**

Toughening mechanisms observed in bioactive glass-ceramics: (a) SEM image of the Vickers indentation in a polished, unetched glass-ceramic; (b) crack bridging; (c) tortuous crack path; (d) crack deflection by the presence of crystalline phase.<sup>[132]</sup>

**Figure 10.**

Mechanical response and toughening mechanisms in the synthetic hybrid composites. (a) SEM image of the structure of nacre; (b) SEM image taken during an in situ R-curve measurement of a lamellar structure; (c) Bending stress-strain curves for the  $\text{Al}_2\text{O}_3/\text{PMMA}$  hybrid materials mimic those of nacre and show >1% inelastic deformation before failure; (d) exceptional toughness for crack growth, similar to that of natural composites, and display significant rising R-curve behavior.<sup>[138]</sup>

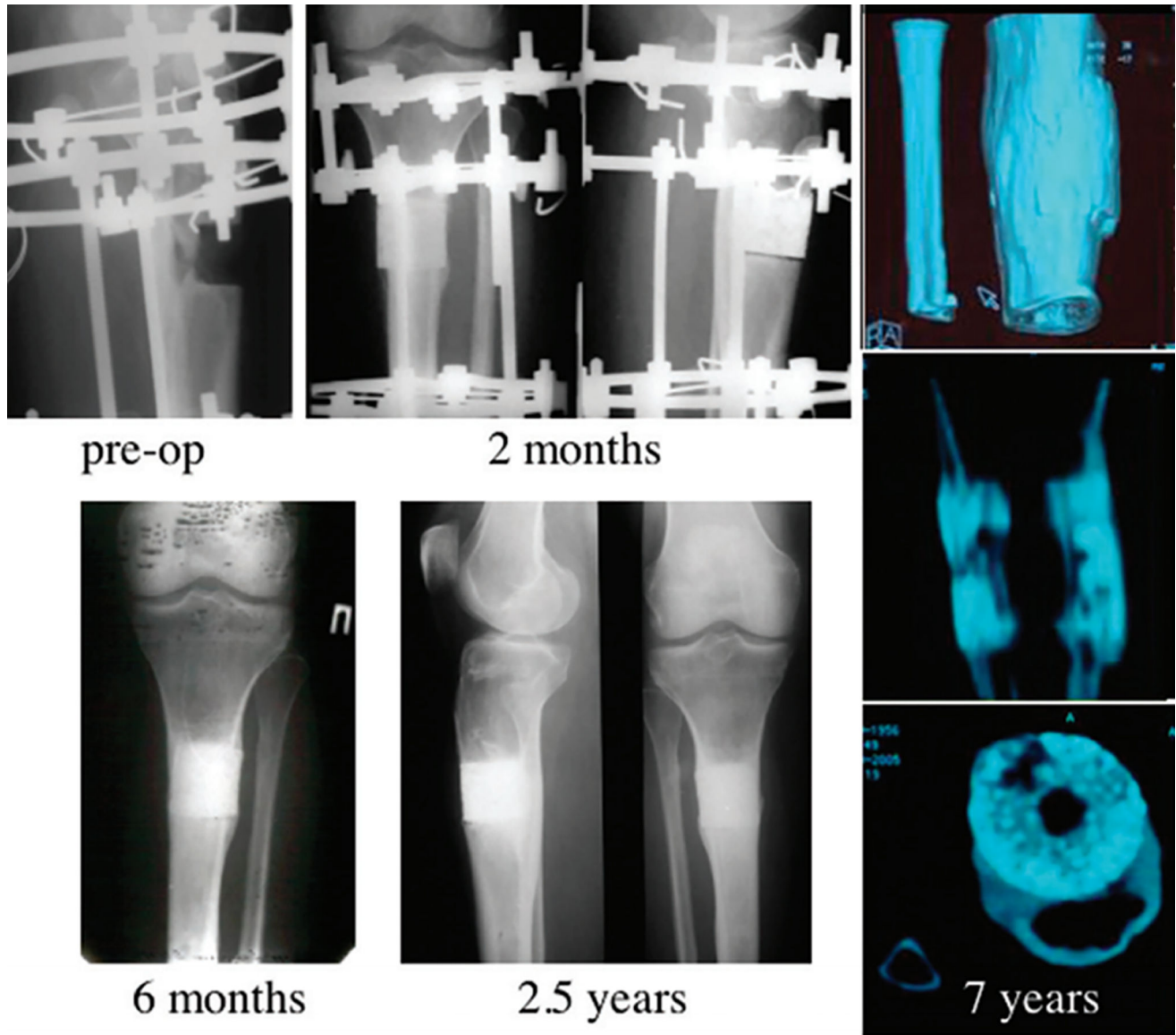


**Figure 11.**

On the preoperative radiograph a 4-cm-long gap of the proximal tibia is shown. At 2 months, bone callus formation around the implant was evident, but the radiolucent line of the bone-implant interface was still detectable in the lateral view. At 6 months, formation of extensive callus and peri-implant bone with a good integration between the implant and the tibia was evident. At 2.5 years follow-up, complete bone-implant integration with no evidence of implant fractures was detected. CT scan analysis at 7 years demonstrated complete healing of the gap, presence of a medullary channel within the implant, and persistence of new bone formation within the bioceramic scaffold pores. The HA ceramic was still present.<sup>[5, 7]</sup>